

# Lawrence Berkeley National Laboratory

## Recent Work

### Title

PHYSICS DIVISION QUARTERLY REPORT, NOV., DEC, 1952 AND JAN. 1953

### Permalink

<https://escholarship.org/uc/item/7vj325rm>

### Author

Lawrence Berkeley National Laboratory

### Publication Date

1953-03-16

UNIVERSITY OF CALIFORNIA - BERKELEY

**TWO-WEEK LOAN COPY**

*This is a Library Circulating Copy  
which may be borrowed for two weeks.  
For a personal retention copy, call  
Tech. Info. Division, Ext. 5545*

**RADIATION LABORATORY**

## **DISCLAIMER**

This document was prepared as an account of work sponsored by the United States Government. While this document is believed to contain correct information, neither the United States Government nor any agency thereof, nor the Regents of the University of California, nor any of their employees, makes any warranty, express or implied, or assumes any legal responsibility for the accuracy, completeness, or usefulness of any information, apparatus, product, or process disclosed, or represents that its use would not infringe privately owned rights. Reference herein to any specific commercial product, process, or service by its trade name, trademark, manufacturer, or otherwise, does not necessarily constitute or imply its endorsement, recommendation, or favoring by the United States Government or any agency thereof, or the Regents of the University of California. The views and opinions of authors expressed herein do not necessarily state or reflect those of the United States Government or any agency thereof or the Regents of the University of California.

UNIVERSITY OF CALIFORNIA

UNCLASSIFIED

Radiation Laboratory

Contract No. W-7405-eng-48

PHYSICS DIVISION QUARTERLY REPORT  
November, December, 1952 and January, 1953

March 16, 1953

Some of the results reported in this document may be of a preliminary or incomplete nature. It is the request of the Radiation Laboratory that the document not be circulated off the project nor the results quoted without permission.

Berkeley, California

## TABLE OF CONTENTS

I.	GENERAL PHYSICS RESEARCH	3
	1. Cloud Chamber Program	3
	2. Film Program	8
	3. Total Proton-Proton Scattering Cross Section at 345 Mev	17
	4. Elastic Proton-Deuteron Scattering (Using 345 Mev Protons)	17
	5. Light Emitted from Argon Under $\alpha$ -Particle Bombardment	18
	6. Progress Report on Technetium Problem	18
	7. Excitation Functions and the Theory of the Compound Nucleus	19
	8. Neutron-Proton Scattering at Small Angles (90 and 270 Mev)	19
	9. Fast Deuterons from 340 Mev Protons on Carbon	19
	10. Internal Momentum Distributions	20
	11. Production of Tritons in Deuteron-Deuteron Collisions	20
	12. Angular Distribution of Charged Mesons Produced by High Energy Neutron Bombardment	21
	13. High Energy Gamma Ray Spectroscopy	21
	14. The Triton Reaction ( $p + d \rightarrow t + \pi^+$ )	22
	15. The Photoproduction of Negative Pions from Deuterium	22
	16. Further Study of Meson Orbits at the 184-inch Cyclotron	23
	17. The Gamma-Gamma Coincidence Detection of Neutral Pions Produced by 340 Mev Protons on Beryllium	24
	18. N-P Scattering Differential Cross Section Near $180^\circ$	25
	19. Low Energy Meson Nucleon Interaction	25
	20. Multiple Small Angle Scattering Measurements	25
	21. Attenuation of Positive Pion in $H_2$	26
	22. Pion Production by Protons on Carbon at $180^\circ$ to the Beam	26
	23. Total Positive Pion Cross Sections in Complex Nuclei	26
	24. Excitation Function for $p + C_{12} \rightarrow \pi^+$	27
	25. Measurements of the Absolute Meson Production Cross Sections	27
	26. Charged Particles from Heavy Elements	28
	27. $p + p \rightarrow d + \pi^+$ Differential Cross Section	29
	28. Beta Ray Spectrometer	29
	29. Time of Flight Neutron Spectroscopy	30
	30. Synchrotron Studies	30
	31. Theoretical Group	31
II.	ACCELERATOR OPERATION AND DEVELOPMENT	35
	1. 184-inch Cyclotron Operation	35
	2. 60-inch Cyclotron Operation and Development	35
	3. Synchrotron Operation	46
	4. Linear Accelerator and Van de Graaff Operation	46
	5. Bevatron Development and Construction	48

\*Previous Physics Quarterly Report UCRL-2054)  
August, September, and October, 1952

## I. GENERAL PHYSICS RESEARCH

### 1. Cloud Chamber Program

Wilson M. Powell

#### The Ten-Atmosphere Wilson Cloud Chamber. J. DePangher

General Features of Construction. Some of the advantages of a high-pressure cloud chamber over one which operates near atmospheric pressure are: (1) tracks are sharper, (2) sensitive time is longer, (3) tracks are rendered more visible because of greater ionization density, and (4) there is a greater density of target nuclei for the incident radiation. A disadvantage which partially offsets (4) in the rate of accumulation of data is that a longer time is required for the gas to become saturated with water vapor.

With these points in mind, a ten-atmosphere cloud chamber with thin windows to admit the neutron beam from the cyclotron was constructed to fit in the six-inch gap of a magnet which provides a field of 21,700 gauss in pulsed operation. In the expanded position of the chamber a cylindrical volume twelve inches in diameter and three inches high is available for the production of tracks. Of this space a region 10.5 inches in diameter and 2.5 inches high is uniformly illuminated for photography.

Figure 1 shows a photograph of the cloud chamber (1) with expansion boxes (2). Each expansion box contains a quick acting valve which is remotely controlled by the magnetic puller (3) through a length of music wire (4). When the cloud chamber is put into the magnet for use with the cyclotron, the pullers are set up just outside the fringing field of the magnet. Air cylinders (5) serve to reset the magnetic pullers following an expansion. The tension in the music wire is adjusted by means of the adjusting screw (6) which serves to slide the puller along the base (7) on which it is mounted.

The main features of the chamber will now be discussed with the aid of Figs. 2A and 2B which employ a common numbering system. Figure 2A displays a drawing of the chamber while Fig. 2B shows an enlargement of a portion of Fig. 2A for the purpose of discussing the thin-window structure.

The central part of the cloud chamber consists of a twelve inch diameter Lucite ring (1) 2 1/2 inches high and 3/4 inch thick. There is located on the top a fully-tempered cover glass (2) (trade name Herculite), 1 1/4 inches thick and with maximum diameter 13 1/4 inches. It is beveled at the edge to set into stainless steel clamping ring (3) so that the latter does not extend above the surface of the glass. Previously, the glass and the stainless steel ring had been assembled and placed in an oven at a sufficiently high temperature so that Wood's metal (4) could be poured into the space between them. This procedure was adopted to insure uniform stress concentration on the cover glass when the clamping ring is attached to the chamber base (5) by means of ten 3/4 inch stainless steel bolts (6). A 1/32 inch thick rubber diaphragm (7) extends horizontally across the cloud chamber and is clamped at the edge between the ridged bottom of the Lucite ring and the circular slot in the chamber base. Beneath the rubber diaphragm and cemented to it a second sheet of

rubber (8) is stretched over the Lucite disk (9), folded over its edge into the "V"-shaped groove provided, and then tied with a number of layers of fish line. The Lucite disk (9), diameter 1 13/16 inches, thickness 1/2 inch, is maintained level at all times by a set of equalizer arms (10) which are fastened to the chamber base.

A preparation consisting of hot water, gelatin and black dye when poured on the surface of the rubber diaphragm soon cools and solidifies and furnishes an excellent background for photography. In addition, it supplies the water vapor that saturates the cloud chamber and serves, when maintained at ground potential, as the lower electrode for the clearing field. The upper clearing field electrode consists of a ring of aquadag which is painted on the bottom side of the cover glass. A small amount of soap when rubbed on the cover glass with the fingers and then polished with cotton permits a thin invisible layer of water to condense on the glass, thus rendering it conducting. A thin copper foil inserted between the cover glass and the Lucite ring allows electrical connection to be made with the aquadag layer from the outside.

To enable the 3/4 inch thick Lucite ring (1) to withstand a gas pressure of ten atmospheres, it was enclosed by a close-fitting stainless steel ring (11) 9/16 inch thick. A series of holes was drilled in the stainless steel so that the light emanating from two flash lamps situated on opposite sides of the chamber can illuminate the active volume in which tracks are formed. After a series of illumination tests had been made with wooden models of the steel ring, a perforation pattern with fifty percent transparency, which resulted in a suitable compromise between the requirements of structural strength and uniform illumination, was selected. Although the Lucite ring could have been made stronger by increasing its thickness, the need for windows of maximum possible area always led to a design in which the Lucite ring alone was structurally inadequate.

Up to 12.5 cm<sup>2</sup> of neutron beam may be admitted through thin windows into the cloud chamber. On the side of the chamber where the neutron beam is to be introduced, a detachable thin-window unit, consisting of a hollow brass frame (12) with thin curved foils (13, 14) of beryllium copper alloy hard soldered to its extremities, penetrates the stainless steel (11) and the Lucite rings (1). The outer foil (13), 0.003 inch thick, is bent into a half-cylinder of diameter 1.25 inches, while the inner foil (14), 0.005 inch thick, is shaped to follow the contour of the inner surface of the Lucite ring. An "O" ring (15) rests in a groove in the brass frame and touches the outer surface of the Lucite ring. Six machine screws which screw into the stainless steel ring (11) force the brass frame (12) against the Lucite so that the "O" ring is compressed to give a pressure seal. In order to reduce the strain on the inner foil (14) (less curved than the outer one) when the cloud chamber is filled with gas at high pressure, gas is introduced into the window cavity and maintained there at a pressure slightly lower than the minimum pressure inside the cloud chamber immediately after an expansion occurs. A second thin-window unit, identical to the one just described, is located on the opposite side of the cloud chamber for the purpose of reducing back-scattering of neutrons.

Gas at regulated pressure is introduced through an inlet (16) into the cloud chamber base (5) to control the expansion ratio. As mentioned previously, two magnetic pullers control symmetrically located expansion valves (17, 18) by means of two lengths of taut music wire (19), 0.029 inch thick, which

pass through small holes in the ends of the expansion boxes (20). During an expansion of the cloud chamber the valves are opened simultaneously to let the gas rush into the expansion boxes while neoprene pads (21) stop the downward motion of the Lucite disk.

The Gas Control System. The gas control system will now be described by referring to Fig. 3. Hydrogen gas, leaving the high-pressure tank (1), passes through a pressure regulator (2), enters the liquid air trap (3), moves through a filter (4) and finally is admitted through a filling valve (5) into the upper volume (6) of the cloud chamber at a pressure  $p_{uv}$ . A vacuum system is not necessary to remove the original gas contained in the upper volume since it is simpler to flush the upper volume a number of times with the aid of the bleed valve (7) until the desired purity of hydrogen is obtained. A precision Bourdon gauge (8), calibrated to an accuracy of  $\pm 0.25$  percent, is provided to measure the pressure  $p_{uv}$ .

Helium gas, leaving the high pressure tank (9), passes through a pressure regulator (10), enters the window cavities (11) and is maintained at a pressure  $p_w$ .

The high pressure system which controls the expansion ratio of the cloud chamber may be described as follows. Five nitrogen tanks (12) (gas pressure 2300 psi when full) are connected through a manifold (13) to a pressure regulator (14). Nitrogen at a pressure 200 psi is stored in the tank (15) which is heated to partly compensate for the cooling of the gas in falling through the large pressure differential. The storage tank (15) contains a large enough volume of nitrogen to sustain a few expansions of the cloud chamber when the tanks (12) become empty and are replaced by full ones. The nitrogen now flows through the precision pressure regulator\* (16) to the "fill lower volume" solenoid valve (17) and then onward to the space beneath the rubber diaphragm which shall henceforth be called the lower volume (18) of the cloud chamber. Let  $p_{lv}$  denote the pressure of gas in the lower volume. A safety valve (19) is provided. Slow expansions are achieved by first closing the "fill lower volume" solenoid valve (17) and then opening the slow expansion valve (20) to let the nitrogen pass through the limit valve (21) into the atmosphere. Before the slow expansion  $p_{lv}$  normally is 148 psi and the limit valve permits it to drop to about 93 psi. When the fast expansion valves (22) are opened, gas rushes into the expansion boxes (23) which contain compressed air at 20 psi pressure.

The gas controls on the expansion boxes may be described as follows. Compressed air at 100 psi from the air compressor (25) passes through the pressure regulator (28), enters the "fill expansion boxes" solenoid valve (29), is warmed at the heater (30) and is maintained at a pressure of 20 psi in the expansion boxes (23). When the expansion valves are opened, the pressure of the air-nitrogen mixture rises to about 78 psi and is reduced to 20 psi by opening the "dump expansion box" solenoid valve (31) and permitting the gas to flow through the limit valve (32) to the atmosphere. For future reference, let  $p_{eb}$  denote the air or air-nitrogen pressure at any time.

Compressed air from the same source (25) emerges from the pressure regulator (26), passes through the "pneumatic reset" solenoid valve (27)

---

\*Moore Products Company, Model 200.



to the air cylinders (24) which reset the magnetic pullers just after an expansion of the chamber is completed.

Table I shows some typical pressures (psig) attained in operating the cloud chamber with hydrogen as the filling gas.

TABLE I

Operation	$P_{uv}$	$P_{lv}$	$P_w$	$P_{eb}$
flushing	5-50-5	0	0	0
filling	0-106	0-93	0-93	0
expansion	147-93-106	148-78	93	20-78

$p_{uv}$  = hydrogen pressure in the upper volume

$p_{lv}$  = nitrogen pressure in the lower volume

$p_w$  = helium pressure in the window cavities

$p_{eb}$  = pressure of the air or air-nitrogen mixture in the expansion boxes

Figure 4 displays a typical cycle of operation for the key valves in the gas control system which has just been described. The time between successive fast expansions of the cloud chamber is two minutes.

Photography. A specially constructed camera is mounted on a light-tight crown 27.5 inches above the cover glass. Pictures are taken through a pair of Leica Summar 50 mm. lenses at f5.6 on Eastman Linagraph Ortho film in 100-foot strips 1.80 inches wide. Two G.E. FT-422 flash-tubes are mounted in light-tight boxes on the sides of the cloud chamber. Two condenser banks, each of capacity 256  $\mu$ f, and charged to 1500 volts, constitute the energy source for the flash-tubes. Light from them, having been rendered parallel by cylindrical lenses made of Lucite, passes through the perforated stainless steel wall of the cloud chamber to the interior. A third lens is used to view a number counter for the identification of each picture and to view an ammeter (see later section on the magnet) which measures the current flowing through the magnet.

Magnet. The cloud chamber is operated in a magnet which, when energized and pulsed with a current of 4000 amperes supplied by a 150 hp. mine-sweeper generator with a five-ton flywheel, furnishes a magnetic field strength of about 21,700 gauss. The maximum variation of the magnetic field over the volume of the chamber in which tracks are photographed does not exceed 2.5 percent. A table, constructed from a uniformity plot of the magnetic field, enables one to determine the field strength at the center of each track measured to an accuracy of  $\pm 0.5$  percent. A large ammeter, used in the calibration of the magnetic field and permanently mounted on the magnet-control cabinet, is read to an accuracy of  $\pm 0.25$  percent each time the magnet

is energized. Although one tries to maintain the magnet current at 4000 amps, occasionally a drift of a few amperes may occur, and so a small correction on the magnetic field is made for this deviation. In case a reading of the large ammeter is missed, one depends on the reading of a smaller ammeter which is recorded on each picture to obtain the magnet current.

Temperature Control. The main body of the cloud chamber is maintained at a temperature of  $19^{\circ}\text{C}$  by a temperature controlled water circulating system in the gap of the magnet. To avoid a temperature gradient developing inside the cloud chamber from gas flow into the lower volume of the chamber, from discharge into the expansion boxes, and from subsequent exhaust into the atmosphere, the gas is pre-heated (see mention of heaters in the section on the gas control system) before it reaches the chamber. A bridge-circuit employing Western Electric thermistors as resistance elements and a Leeds and Northrup Micromax Recorder, ten millivolts full scale, records the temperature difference between the top and bottom of the chamber. In the course of a long run the bottom becomes colder than the top but the temperature control is adequate to keep the temperature difference below  $0.5^{\circ}\text{C}$  (about 0.5 millivolts deflection on the recorder).

Synchronization of Cloud Chamber, Magnet and Cyclotron. The timing system consists of (1) a "slow timer", (2) a fast timer and (3) an oscilloscope for measuring time intervals.

The slow timer controls the solenoid valves in the gas control system that perform the following operations: (1) fill lower volume, (2) slow expansions, (3) fill expansion boxes, (4) dump expansion boxes and (5) pneumatic reset. The valves are either manually controlled by toggle switches, or automatically operated by microswitches which are resting on cams driven by a variable speed d.c. motor. In addition, the slow timer activates the film-wind mechanism, turns on the magnetic field, and operates a time delay which in turn triggers the fast timer.

Vacuum tube operated relays in the fast timer perform such operations as (1) shorting out the clearing field just before an expansion of the cloud chamber, (2) flashing lights which illuminate the number-counter and the magnetic field current meter, (3) starting the fast expansion, (4) pulsing the cyclotron, and (5) initiating the condenser discharge through the flash-tubes. An adjustable RC-network in the grid circuit of each vacuum tube (6SN7) allows a time-range-control up to 200 milliseconds.

It takes about 2.5 seconds for the magnet current to reach the value 4000 amperes, where it remains steady for about 0.2 second before being turned off. The time delay on the slow timer is adjusted so that the fast expansion is completed during the steady period of the magnet current. A few milliseconds later the cyclotron is pulsed three times and the neutron beam is admitted to the cloud chamber. Fifty milliseconds after the third pulse of neutrons has entered the chamber, the lights are flashed. In this way, pictures of proton-recoil tracks produced in hydrogen are very sharp and practically free from turbulence.

One views timing signals from the rapid succession of events just described on an oscilloscope with persistent screen. The horizontal time sweep is triggered at the instant the slow timer starts the fast timer. Timing marks for calibration of the horizontal sweep are spaced  $1/60$  second apart.

The following signals, after passing through a pulse-shaping circuit, appear on the vertical sweep: (1) signals from the relays in the fast timer which initiate the fast expansion and the condenser discharge through the flash-tubes, (2) a signal from a switch called the bottom switch in the chamber base (this switch is closed when the expansion is completed), and (3) signals from a counter responding to the cyclotron pulses. Figure 5 shows graphically the succession of events which occur when the cloud chamber is operated with the cyclotron.

## 2. Film Program

Walter H. Barkas

### Physical Analysis of Be and C Disintegration Induced by 330 Mev Protons. W. H. Barkas and H. Tyren

The disintegration products of carbon and beryllium emerging from thin targets bombarded by an internal cyclotron beam of 330 Mev protons have been studied. The magnetic field of the cyclotron is employed for momentum analysis and nuclear track plates for detection and range analysis. On plotting radius of curvature versus range, various nuclear species are found to fall on identifiable loci. The relative abundances of the products and their momentum spectra are obtained. Hydrogen, helium, lithium and boron products have been found, and their abundances tabulated. Alpha particles prove to be the most important charged particle product. Beryllium yields significantly more tritium than carbon. Some of the heavy products are found with very high momenta.

### A Test of the Charge Symmetry Hypothesis. H. W. Wilson and W. H. Barkas

When alpha particles bombard carbon, for every process leading to the emission of a positive meson there exists a mirror process leading to the emission of a negative meson. If the charge symmetry hypothesis is valid, one would therefore predict a plus/minus ratio of unity for pion production under the conditions where the coulomb barrier can be neglected. An experimental arrangement was employed to measure this ratio which eliminates to a large extent the known sources of systematic error. For mesons of nominal energy 15 Mev (total spread 11-21 Mev), the plus/minus ratio from carbon for mesons emitted at  $90^\circ$  to the 375 Mev alpha particle beam was found to be 0.72 with a standard deviation of 0.17. Estimation of the expected depression of the ratio caused by coulomb effects has been made<sup>1</sup>. It is concluded that the measured ratio agrees within its standard deviation with that anticipated on the basis of the charge symmetry hypothesis. Another experiment which attempted to utilize mesons of  $\approx 30$  Mev failed because the obtainable meson flux was too low. With the same apparatus the plus/minus ratio for pions emitted at  $90^\circ$  to a 330 Mev proton beam bombarding carbon was measured. A ratio of  $5.4 \pm 0.8$  was found.

---

1. B. Fried and S. Gasiorowicz, private communication.

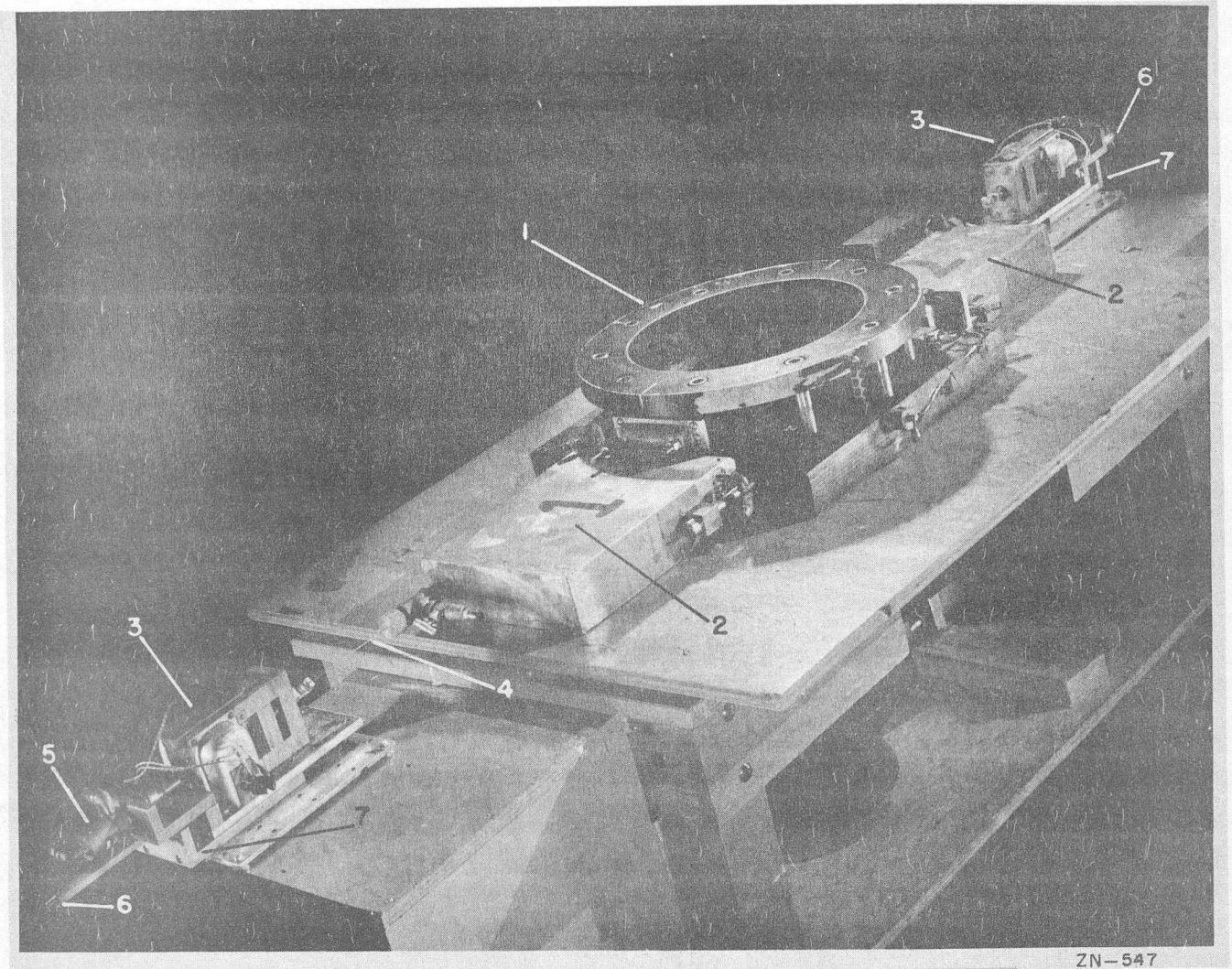
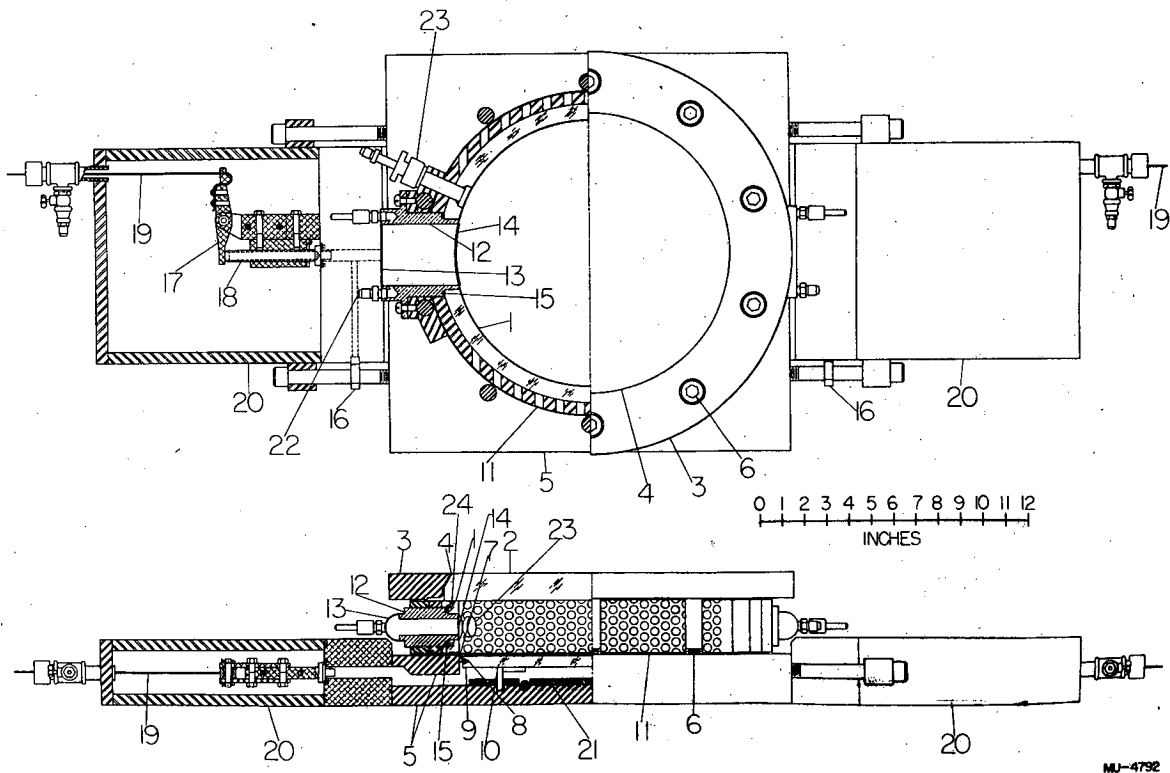


Fig. 1  
Photograph of ten-atmosphere cloud chamber assembled with expansion boxes and magnetic pullers.

Fig. 1

Photograph of ten-atmosphere cloud chamber assembled with expansion boxes and magnetic pullers.



MJ-4792

Fig. 2A  
Drawing of the ten-atmosphere cloud chamber.

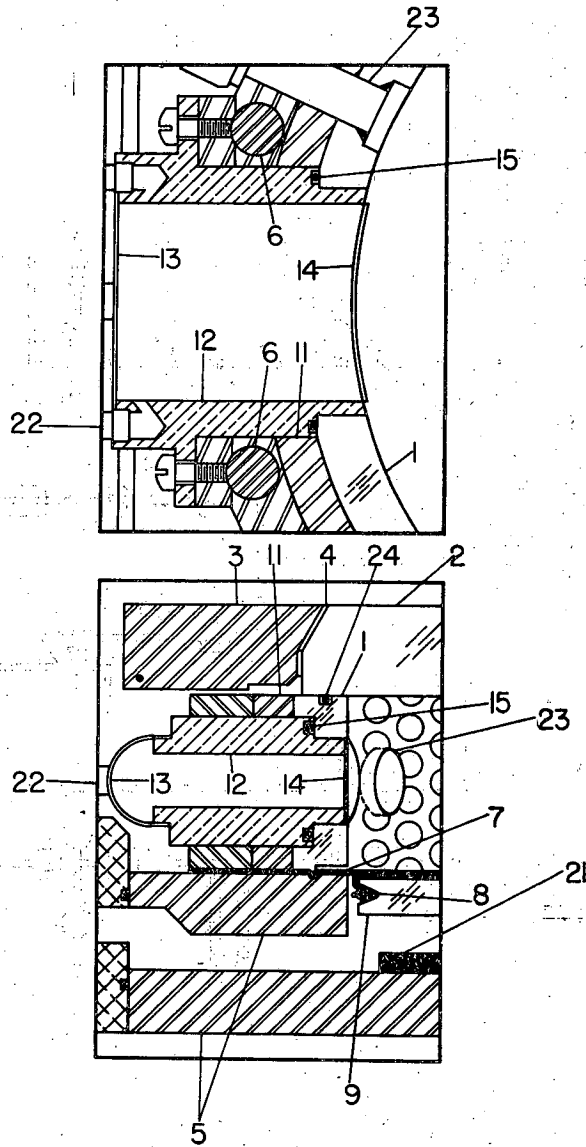
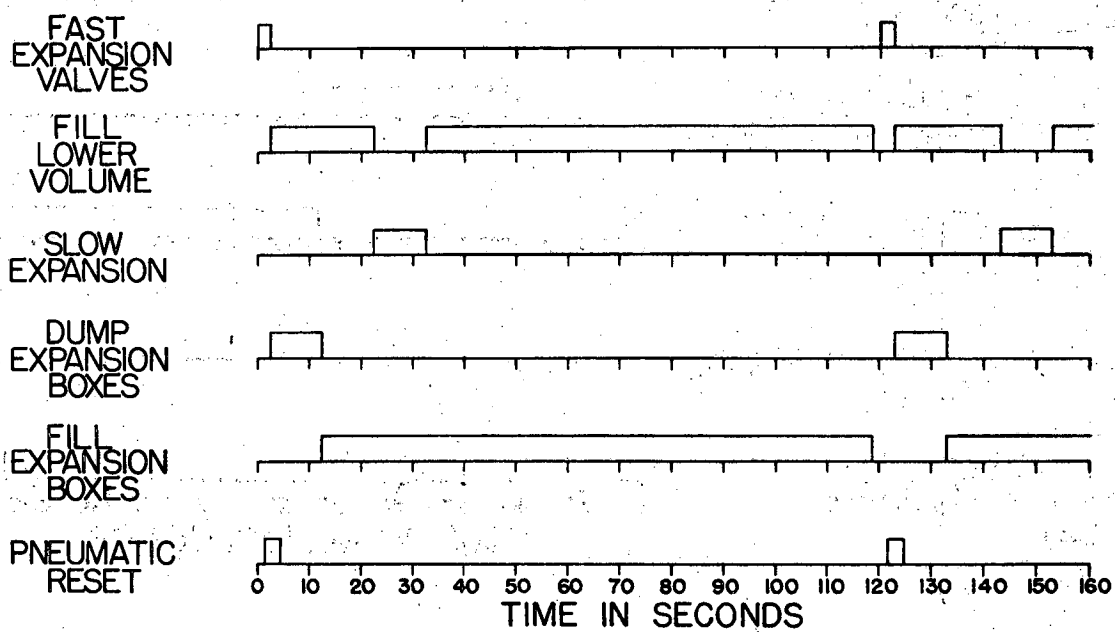


Fig. 2B

An enlargement of a portion of Fig. 2A for the purpose of showing the thin window structure.



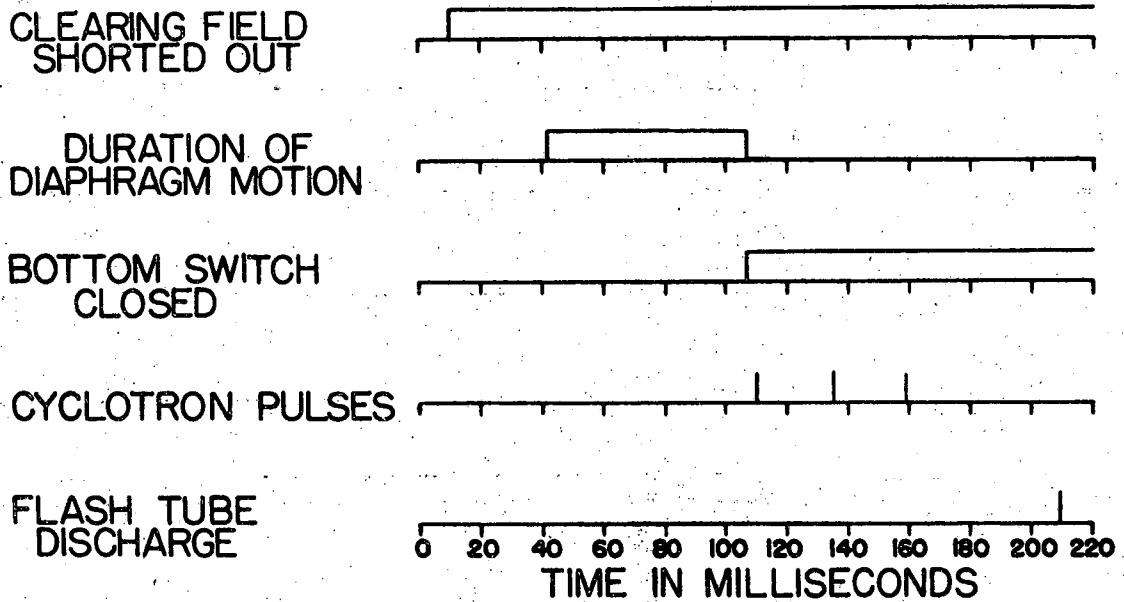


MU-4777

Fig. 4

Typical cycle of operation of the electrically-operated valves in the gas control system.





MU-4794

Fig. 5

Succession of events occurring when the cloud chamber is operated with the cyclotron.

The Range Correction for Electron Pick-up. W. H. Barkas

The extension of positive particle ranges caused by pick-up of electrons at low velocities has been studied in Ilford C2 emulsion. Ranges of  $\text{Li}^8$  and  $\text{B}^8$  nuclei were measured in emulsion and compared with tracks of helium and hydrogen isotopes of the same velocity. The empirical range-energy relation adduced for light nuclei is:

$$\frac{Z^2 R}{M} = F \left( \frac{T}{M} \right) + 0.46Z^2 + 0.0063 Z^4$$

Production of Negative  $\mu$ -Mesons and Their Behavior in Nuclear Research Emulsions. Dora F. Sherman

A beam of negative  $\mu$  mesons produced inside the tank of the 184-inch cyclotron has been studied.  $3 \pm 1$  percent formed one prong stars when stopped in Ilford C2 emulsion. Two two-prong stars with prong ranges of 2 or 3 microns were observed which appear to be fission-like disintegrations induced by  $\mu^-$  capture. 32 percent of the  $\mu^-$  mesons have clusters of grains about 1 micron in diameter or two pronglets about one micron long at their termini. These are interpreted as Auger electrons accompanying capture by a heavy nucleus, or in some cases as fission of the capturing nucleus. An upper limit on the cross section for direct production of negative  $\mu$  mesons,  $d\sigma/d\Omega dp$ , in the forward direction at  $pc = 129$  Mev, has been evaluated to be 0.015 times the cross section for production of negative  $\pi$  mesons in the same interval.

Variation of Moisture Content in Nuclear Track Emulsion. A. J. Oliver

Ilford emulsions for nuclear research, both unprocessed and processed, have been brought to equilibrium with different relative humidities and then measured in thickness, volume, and weight. The variation of emulsion volume and weight with time in a vacuum, for different thicknesses of unprocessed emulsion on glass, has been followed. Moisture diffusion rates through the emulsion and the non-linear relationship between thickness and water content have been investigated. Thicknesses were measured by a dial indicating micrometer. Volumes were measured by displacement. Humidities were maintained in some cases by salt solutions and in others by aqueous solutions of glycerine. New values have been computed for emulsion density and for the dependence of the shrinkage factor on relative humidity and processing procedure.

Secondary Particles Induced by 375 Mev Alpha Particles. R. W. Deutsch and W. H. Barkas

Thin targets of Be, Al, Ni, Ag, Au, and U have been bombarded by an internal cyclotron beam of 375 Mev alpha particles. Secondary particles emerging from the disintegration of the nuclei are detected in Ilford C2 nuclear track plates located beneath the median plane of the cyclotron. There are three specific positions for the nuclear plates corresponding to mean proton energies of about 5, 10, and 20 Mev. A secondary particle is identified by measurement of its radius of curvature, range, and specific ionization. The light secondaries including  $\text{H}^1$ ,  $\text{H}^2$ ,  $\text{H}^3$ ,  $\text{He}^3$ , and  $\text{He}^4$  fall on identifiable loci. Heavier fragments are also identified by taking into account electron pick-up<sup>1</sup>. Relative abundances of the secondary particles and momentum spectra are obtained.

---

1. W. H. Barkas, UCRL-1937.

## $\pi^+/\pi^-$ Ratios Measured with the Use of the Spiral Orbit Spectrometer. R. Sagane

The results of the experiment, preliminarily reported earlier<sup>1</sup>, are as follows: The  $\pi^+/\pi^-$  ratios for mesons produced by 345 Mev protons at 90° for energies  $13 \pm 4$  Mev,  $18 \pm 4$  Mev, and  $41 \pm 2$  Mev have been obtained. The ratios are: Be ( $1.3 \pm 0.4$ ,  $5.2 \pm 1.3$ ,  $5.8 \pm 1$ ); C (---,  $5.0 \pm 1$ ,  $11.5 \pm 2.5$ ); and Al ( $4 \pm 0.8$ ,  $2.5 \pm 1.2$ ,  $1.6 \pm 0.4$ ), respectively. Plates for Cu, Ag and Pb are now being scanned.

Several developmental tests for the use of the spiral orbit spectrometer have been made. The following items will be discussed. (1) The vertical focusing is working favorably and it is possible to adjust this effect. (2) The energy resolution of the spectrometer was usually too high compared with the energy spread caused by absorption through the targets. It is possible to reduce the resolution by adding annular ring pole pieces and increase the intensity. (3) To reduce energy spread due to absorption both for mesons and protons, thin walled conical or tubular targets were used. (4) The projected range straggling curve of 8 Mev mesons in C2 emulsion was obtained. This enables one to calculate the absolute number of mesons arrived at the detector.

## Large Angle Scattering of Negative Pions in Aluminum, Copper and Lead. H. H. Heckman

A new technique is used to measure the cross sections for large angle scattering of negative pions as they traverse a semi-infinite scatterer. A stripped emulsion is embedded in the scatterer, exposed to an incident beam of  $50^{+15}_5$  Mev  $\pi^-$  mesons, and scanned. Most of the mesons stop at the expected distance from the absorber edge as determined from the range-energy relation. A few mesons are found at smaller depths of penetration and are attributed to large angle scattering. Star forming mesons that enter the emulsion traveling opposite ( $90^\circ$  -  $180^\circ$ ) to the direction of the incident beam are attributed to nuclear backscattering and are used in the cross section calculation. This method affords an effective solid angle of  $2\pi$  steradians for observing nuclear backscattering. The cross section is proportional to the ratio of backward flux to incident flux, both of which are observed in the same strip of emulsion. The conclusions of this investigation are: a) The scattering of negative pions from complex nuclei is consistent with energy independence in the region of  $32 \pm 10$  Mev. b) The S- and P-waves contribute to backscattering. c) The cross section for backscattering is proportional to the mass number, A, which indicates that pion - nucleon collisions are observed. The calculations of the cross sections include corrections for inelastic collisions. The total nuclear backscattering cross sections (elastic and inelastic) for negative pions in aluminum, copper, and lead are  $59.6 \pm 11$  mb.,  $192 \pm 27$  mb., and  $577 \pm 80$  mb., respectively.

## Other Researches.

Progress has been made on the following additional researches: Meson spectrometer magnets; measurement of meson masses and the energy balance in meson decay; measurement of meson spectra; measurement of high energy beta ray spectra; and study of high energy electron processes.

---

1. R. Sagane and P. C. Giles, Phys. Rev. 81, 653 (1951).

### 3. Total Proton-Proton Scattering Cross Section at 345 Mev

O. Chamberlain, E. Segrè and C. Wiegand

It is still proposed to measure the total p-p scattering cross section by attenuation in a liquid hydrogen target of thickness about  $4 \text{ gr/cm}^2$ . The experiment has been hampered by an unusual amount of difficulty in eliminating leaks from the liquid hydrogen dewar.

At present there is some hope that the experiment may soon be making reasonable progress, since the dewar has seemed tight in a brief test with liquid hydrogen. Other parts of the apparatus have been rather thoroughly tested some months ago and are believed in fairly good working order.

### 4. Elastic Proton-Deuteron Scattering (Using 345 Mev Protons)

D. D. Clark and O. Chamberlain

The measurement of cross sections in this experiment requires a method of particle detection which can identify the scattered particles as either protons or deuterons; as has been described previously, measurement of specific ionization and of total energy by means of photographically recorded pulse heights in a thin and thick counter respectively is the identification method which has been chosen.

For deuterons of high energy two liquid scintillators of about 1.8 and  $13.9 \text{ gm/cm}^2$  copper equivalent have been employed for measurements at several center of mass angles. A considerable amount of data from a recent run has not yet been read from the film, but a tentative center of mass cross section for  $70^\circ$  (center of mass) can be reported:  $0.028 \pm 0.0085$  millibarns/steradian. No systematic errors have been included.

For deuterons of low energy a thinner  $dE/dx$  counter is necessary and is under construction.

The technique has proved itself adequate and reliable and it is expected that accumulation of sufficient data will be the only problem remaining in the completion of the experiment.

It had been expected that the deuteron background from the carbon in the  $(\text{CD}_2)_n$  targets employed would be negligible, as p-d elastic events are identified by the production of a deuteron in coincidence with a charged particle detected in a counter on the other side of the beam. However, such deuterons from carbon were observed in several cases. A postulated process is a nucleon-nucleon event inside the carbon nucleus, followed by a pickup of another nucleon by the scattered particle to form a deuteron. This hypothesis has not been tested yet but has been independently discussed in a theoretical article by Bransden in Proc. Phys. Soc. (London), 65, 738 (1952).

## 5. Light Emitted from Argon Under $\alpha$ -Particle Bombardment

E. Segrè and C. Wiegand

With the hope of finding a scintillator that would emit an amount of light proportional to the energy spent by a fission fragment in it an attempt was made to see the light emitted by argon gas under alpha particle bombardment. In a plane parallel condenser full of argon alphas from Po were shot and the gas was "looked" at with a 5819 photomultiplier.

The following facts were found; 1) Light was emitted when an electric field was applied to the gas. 2) The amount of light per alpha was roughly proportional to the potential difference between the plates of the condenser. 3) The amount of light was approximately independent of the argon pressure between 0.5 and 2 atmospheres. 4) The light was suppressed by small amounts of impurities such as CO<sub>2</sub>, O<sub>2</sub>, N<sub>2</sub>, etc. 5) The light was emitted during a time comparable with the time of motion of the electrons in the condenser. This time was measured by displaying on the same oscilloscope sweep the output of the 5819 and the ionization current produced by the alphas in the gas.

A partial explanation, which however is subject to some criticism is that the electrons move in the condenser making elastic collisions with the argon until they reach a critical energy sufficient to excite it. They undergo then an inelastic collision after which they resume the cycle. The facts enumerated above are all in agreement with this simple explanation, but the level structure of the argon atom offers some difficulties which we hope to clear up by studying the spectrum of the light emitted.

## 6. Progress Report on Technetium Problem

E. Segrè and T. J. Ypsilantis

The search for long lived technetium isotopes in ores is continuing. Recently there was received a shipment of four different ore concentrates from Kenecott Copper Corporation. These concentrates have been treated so as to concentrate the rhenium and technetium, using short lived artificial Tc tracers to test the chemical techniques. The enriched products are now awaiting spectroscopic analysis for detection of naturally occurring technetium, if present.

Experiments attempting to achieve preferential reduction of rhenium in the presence of technetium have been attempted with little success as yet. Further experiments are planned using a Jones reductor. Determinations of the distribution coefficient of rhenium vs. technetium in the precipitation of K Re O<sub>4</sub> under varying conditions of temperature and mixing are still in progress.

## 7. Excitation Functions and the Theory of the Compound Nucleus

Walter John

The Ghoshal experiment (Phys. Rev. 80, 939 (1950)) provided an experimental test of the compound nucleus theory. The excitation functions for  $\text{Ni}^{60} + \alpha$  were compared to those for  $\text{Cu}^{63} + p$ . The compound nucleus formed in each case was  $\text{Zn}^{64}$ . It is now found that the comparison of the excitation functions for  $\text{Bi} + p$  and  $\text{Bi} + \alpha$  (Kelly, Phys. Rev. 75, 999 (1949)) also confirms the compound nucleus theory. Here the compound nucleus is not the same; however, by a suitable shift of the energy scales the curves fit remarkably well. It is found that the required energy shift is just the difference in thresholds of corresponding reactions. This is equivalent to the requirement that the residual nucleus in each case is left with the same excitation, which is in agreement with the theoretical prediction of Weisskopf.

Preparations are being made for the measurement of the excitation functions obtained from bombarding Pb with  $\alpha$  particles. These functions will be compared to the Bi excitation functions as a further check on the theory. These considerations may be of considerable practical importance since it may prove possible to utilize these comparisons to predict excitation functions from the known excitation functions.

## 8. Neutron-Proton Scattering at Small Angles (90 and 270 Mev)

J. Easley and G. Pettengill

Trial runs thus far have indicated that there will be adequate intensity with sufficiently low background to make the experiments for center of mass angles of 20 degrees to 60 degrees. There are indications that these measurements may be extended to somewhat smaller angles.

At the present time the replacement of one of the counters has very nearly been completed, and some additional shielding to be placed adjacent to the neutron beam is expected to be available from the shops very soon.

## 9. Fast Deuterons from 340 Mev Protons on Carbon

W. N. Hess and John Wilcox

It has been decided to use the 35 channel magnetic particle spectrometer already described in these reports to investigate the energy spectrum of deuterons having energies above 20 Mev produced when 340 Mev protons bombard various elements. The first experiments will be done looking at deuterons at  $40^\circ$  to the beam direction. Few deuterons from the pick-up process should be seen at this angle. However, a second order process called the indirect pick-up process<sup>1</sup> can contribute deuterons at this angle. The deuteron energy spectrum should be peaked at about 50 Mev. The magnetic particle

---

1. B. H. Bransden, Proc. Phys. Soc. A 65, 738 (1952).

spectrometer separates particles according to their momenta. Deuterons and protons having the same momentum differ in range by about a factor of five. They can easily be separated by introducing a wedge-shaped absorber into the spectrometer which will absorb the deuterons.

A preliminary run indicated that there are few, if any, deuterons having energies above 100 Mev but that deuterons were present in the energy range 40 to 150 Mev. Probably about 10 percent of the counts in momentum channels corresponding to these energies were deuterons.

## 10. Internal Momentum Distributions

John Wilcox and W. N. Hess

The 35 channel scintillation counter rack has been completed and tested in several runs. Certain modifications have been made in the associated gated amplifiers to convert them from geiger to phototube operation. Timing difficulties have been overcome by adding 1.3 microsecond delay boxes to each channel.

The scattered incident proton and the proton knocked out of the nucleus have been detected in coincidence using a quadruple coincidence circuit with a resolving time of  $3 \times 10^{-9}$  sec. developed by Dr. Madey. One crystal in the spectrometer arm is made one-fourth inch wide to serve as the defining slit.

Rough data have been obtained for polyethylene, lithium, beryllium and carbon with the method of observing one partner in the collision only. These indicate that the 35 channel detection efficiencies must be made more uniform.

## 11. Production of Tritons in Deuteron-Deuteron Collisions

Charles Godfrey

The reaction  $d + d \rightarrow H^3 + p$  was studied using 190 Mev deuterons in the cave. Fast pulses from stilbene scintillation counter telescopes were employed to get coincidence counts between the two outgoing particles. Range and time-of-flight methods were used to reduce the effective background. It was found quite feasible to run at full beam strength. The process was first identified by: (1) moving the triton telescope in azimuth and elevation; (2) inserting a delay of  $5 \times 10^{-9}$  sec. between coincidences; and (3) inserting enough absorber to just stop the postulated particle. In all cases the net counting rate substantially disappeared. Values of the differential cross section at  $45^\circ$ ,  $60^\circ$  and  $90^\circ$  (center-of-mass) were obtained. The cross section at  $90^\circ$  is approximately  $10 \mu$  barns and is rising very steeply at  $45^\circ$ . This behavior is not unexpected if one postulates a strong pick-up process to dominate the cross section mechanism.

## 12. Angular Distribution of Charged Mesons Produced by High Energy Neutron Bombardment

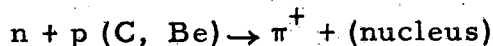
Lee Neher

The experimental results for the angular distribution of  $\pi^-$  mesons from carbon and beryllium targets show a symmetry about  $\theta = 90^\circ$  when transformed to an average center-of-mass (c.m.) frame, with  $\beta_{cm} = 0.27$ . If one takes the beryllium  $\pi^-$  cross section and subtracts two-thirds of the carbon cross section per nucleus, the effect due to the "extra" neutron ( $n'$ ) in beryllium is obtained. The c.m. data can be fitted with a  $B(A + \cos^2 \theta)$  curve. The neutron beam intensity was monitored by an  $n \rightarrow p$  scattering monitor. It is possible to assign absolute average cross sections to the above results. The mean neutron energy for  $\pi$  meson reaction is 310 Mev for the 184-inch cyclotron neutron beam.

Postulated Reaction	A	B
$n + n \text{ (Carbon)} \rightarrow \pi^- \pm d + C^{11}$	$0.49 \pm 0.08$	$2.35 \pm 0.20 \times 10^{-28} \text{ cm}^2 \text{ st}^{-1} \text{ nucleus}^{-1}$
$n + n \text{ (Be)} \rightarrow \pi^- \pm d + Be^8$	$0.28 \pm 0.05$	$2.90 \pm 0.19 \times 10^{-28} \text{ cm}^2 \text{ st}^{-1} \text{ nucleus}^{-1}$
$n + n' \text{ (Be)} \rightarrow \pi^- \pm d + Be^8$	$0.12 \pm 0.06$	$0.92 \pm 0.14 \times 10^{-28} \text{ cm}^2 \text{ st}^{-1} \text{ neutron}^{-1}$

The  $\pi^+$  meson angular distribution appears to be the same from C or Be and is nearly constant in the average c.m. system.

Our best estimate for the reaction



in the same average c.m. system is

$$\left[ \frac{d\sigma}{d\Omega} \right]_{\pi^+} = \left[ (6.1 \pm 2.2) - (0.03 \pm 0.02) \theta \right] \times 10^{-30} \text{ cm}^2 \text{ st}^{-1} \text{ nucleus}^{-1}$$

The data suggests that  $\pi^-$  production by high energy neutrons is similar to  $\pi^+$  production by high energy protons in both magnitude and angular distribution of the mesons in a center-of-mass system. Details of the experiment will appear soon in an UCRL Report.

## 13. High Energy Gamma Ray Spectroscopy

David Cohen, Harlen Shaw, and Charles Waddell

A run was recently made on the synchro-cyclotron with the pair spectrometer modified so as to cover photon energies from 10 Mev to 200 Mev. The target was carbon and the particle beam was protons. The data from this apparatus are still on a tentative basis as the various characteristics of the apparatus are being identified. In the recent run the  $\pi^0$  gamma spectrum from



340 Mev protons was examined from 10 Mev upwards in energy and provides a continuous band of analyzed photons from the region of nuclear gamma rays up to the region of  $\pi^0$  gamma rays. A strong nuclear line was observed between 15 and 18 Mev, which can presumably be associated with the 17 Mev photons from the excited lithium nucleus.

The proton target was subsequently placed at smaller cyclotron radius, below the  $\pi^0$  threshold, and the bremsstrahlung spectrum from bombardment by 150 Mev protons was analyzed. The nuclear gamma line referred to above was again seen, superimposed on what may be a characteristic bremsstrahlung spectrum whose intensity is regularly decreasing with increasing energy.

#### 14. The Triton Reaction ( $p + d \rightarrow t + \pi^+$ )

Kenneth Bandtel, James Frank, Richard Madey and Burton J. Moyer

Further data on the angular distribution of the reaction  $p + d \rightarrow t + \pi^+$  was obtained in a two-day run this quarter. Preliminary results for pion angles of  $30^\circ$ ,  $50^\circ$ ,  $70^\circ$ ,  $90^\circ$ ,  $130^\circ$  and  $150^\circ$  in the center of momentum system show a peak in the forward direction and a flat distribution in the backward direction. The ratio of  $\frac{d\sigma}{d\Omega}(0^\circ)/\frac{d\sigma}{d\Omega}(90^\circ)$  is about six. The estimated total cross section is around five microbarns.

Ruderman<sup>1</sup> has calculated an angular distribution by viewing the reaction as a two-step process: first, a  $p + p \rightarrow d + \pi^+$  reaction occurs between the incident proton and the proton in the deuteron; second, the newly formed deuteron picks up the left over neutron to form a triton. The first step imposes a  $\cos^2\theta$ -type distribution, while the second reduces the backward peak relative to the forward peak. This asymmetry comes from the internal momentum distribution in the target deuteron. Bludman is continuing the theoretical analysis; he thinks that by using a hard core model of the nucleon, the deuteron internal momentum distribution might be modified in such a way as to flatten out the backward peak.

#### 15. The Photoproduction of Negative Pions from Deuterium

Kenneth Bandtel, James Frank and Richard Madey

The negative pions and protons were detected in coincidence. Two pion counters and one proton counter were connected in triple coincidence with a resolution time and a dead time of  $3 \times 10^{-9}$  seconds. The laboratory proton counter angle was  $20^\circ$  and the laboratory pion telescope angle was  $120^\circ$ . The proton counter was 31.5 inches from the target and the second pion counter was 14.3 inches from the target. This geometry allows the relatively slow protons to be separated from the  $\beta = 1$  electron background by time-of-flight dispersion.

---

1. Phys. Rev. 87, 383 (1952).

Targets of  $CD_2$ ,  $CH_2$  and C were designed to contain an equivalent number of carbon atoms. Copper absorber was used in the pion telescope to stop low energy charged particle background and to increase the energy loss of the pions. When this absorber was placed in front of the pion telescope, both the  $CD_2 - CH_2$  and  $CH_2 - C$  difference counting rates were found to be real. The  $CD_2 - CH_2$  difference counting rate corresponds to bombarding the neutron with a  $\gamma$ -ray and making a proton-negative pion coincidence. The  $CH_2 - C$  difference corresponds to bombarding the proton with a  $\gamma$ -ray and making a proton-photon coincidence. This latter process has very nearly the same angular correlation as that for the proton and negative pion. When the copper absorber was placed between the two pion counters, then the  $CH_2 - C$  difference counting rate nearly disappeared while the  $CD_2 - CH_2$  difference counting rate remained the same. The reason is that the photon cannot be converted by the copper absorber until after it has passed through the first pion counter without causing a coincidence. The first counter is a very small fraction of a radiation length, while the thickness of the copper absorber varies for the conditions of the experiment from one to two radiation lengths; hence, very few  $\gamma$ -rays are converted in the first pion counter.

The pion scope "feed-through" problem, discussed in the last quarterly report, has been eliminated by a slight modification of the coincidence circuit.

The high energy end of the negative pion spectrum has been studied. These data are now being analyzed in detail to see if a measure of the nucleon spin flip probability in the reaction  $\gamma + d \rightarrow \pi^- + 2p$  can be ascertained.

#### 16. Further Study of Meson Orbits at the 184-inch Cyclotron

The detection of an available flux of negative  $\pi^-$  mesons just outside the tank wall of the 184-inch cyclotron was described in the last quarterly report. The observed orbits appeared to be in rough agreement with those calculated by Barkas and Rankin at an earlier date.

Before certain experiments could be performed, however, it was deemed necessary to explore the meson trajectories for various energies and various angles of emission by means of the flexible wire technique. The results of this exploration indicated that the present features of the target support and the thin window for emergence of the mesons allow an energy region extending from about 60 Mev up to the upper energy limit of the mesons created to emerge. In the region of 70 Mev there is a quasi-focusing of the trajectories so as to yield a fairly well defined parallel flux of mesons of this energy in a beam whose cross sectional area is roughly four square inches. A few modifications of the meson target support and of the thin window frame will allow mesons of lower energies to emerge into the accessible region of the platform.

17. The Gamma-Gamma Coincidence Detection of Neutral Pions  
Produced by 340 Mev Protons on Beryllium

Richard Madey, Kenneth Bandtel and James Frank

Previous work on this experiment was done with  $2 \times 10^{-8}$  second dead time and resolution time scintillation counting equipment. Background from the target prevented running at a beam intensity that would give reasonable counting rates. Two runs were made this past quarter. The first run was made with  $3 \times 10^{-9}$  second dead time and resolution time scintillation counting equipment; the second run was made with two water-filled Cerenkov counters.

The background from a  $2 \frac{1}{8}$  inch thick beryllium target with the  $3 \times 10^{-9}$  dead time equipment was smaller than that with the  $2 \times 10^{-8}$  second dead time equipment. For the first time, the quadruple coincidence counting rate per unit of integrated beam was on a plateau with respect to beam intensity; however, background from the target still limited the usable beam intensity. The difference in the counting rates with one-fourth inch lead and five-fourths inch carbon converters is about 1.5 counts per minute at a beam intensity just below the knee of the plateau region.

The second run with two Cerenkov counters was more successful. A water medium was chosen for the Cerenkov counters because the index of refraction of water is low enough to prevent the generation of Cerenkov radiation by the passage of protons. Since a charged particle is required to produce Cerenkov radiation, the notoriously large neutron background associated with the external proton beam would be discriminated against by Cerenkov counters. With two Cerenkov counters connected in double coincidence, the background was not eliminated. The gamma-gamma coincidence counting rate (per unit of integrated beam) increased linearly with an increase in the beam intensity of a factor of ten. A small extrapolation to zero beam intensity clearly gave a non-zero intercept. In order to study the nature of the background lead transition curves were obtained at two values of the beam intensity. Analysis of these two lead transition curves showed that the background gamma rays are of nuclear origin with a very crudely estimated cross section of around 0.3 barn.

The angular correlation of the decay photons was measured at neutral pion production angle of  $90^\circ$ . The result is in agreement with the kinematical relationship appropriate to neutral pion disintegration into two photons. The relative gamma-gamma coincidence counting rates for correlation angles of  $45^\circ$ ,  $90^\circ$  and  $180^\circ$  are in good qualitative agreement with similar relative counting rates for photon produced neutral pions<sup>1</sup>. The principal difference is that the relative counting rate at a correlation angle of  $180^\circ$  is larger for the case of proton bombardment than for the case of the photon bombardment. This result indicates that the spectrum of neutral pions produced at  $90^\circ$  to the beam contains relatively more low energy neutral pions when a beryllium target is bombarded by 340 Mev protons than when it is bombarded by 320 Mev bremsstrahlung spectrum.

---

1. Phys. Rev. 86, 180 (1952), W. K. H. Panofsky, J. N. Steinberger, and J. Steller.

The difference in the double coincidence counting rates with one-fourth inch lead and five-fourths inch carbon converters, at a correlation angle of  $90^\circ$ , was  $3.7 \pm 0.4$  per minute for a value of the beam intensity where the background counting rate was about one-quarter of the neutral pion counting rate. This counting rate is in good agreement with the calculated counting rate, if the cross section of Crandall<sup>2</sup> for neutral pion production from carbon is used.

### 18. N-P Scattering Differential Cross Section Near $180^\circ$

L. Kerth and B. Youtz

The n-p scattering differential cross section has been measured at 90 Mev and 310 Mev for c.m. scattering angles between  $139^\circ$  and  $176^\circ$ . The cross sections for 7 angles were measured in this angular range, using the annular ring target and counter system of W. Ball (thesis) with standard deviations due to counting statistics of two to four percent. In each case, normalization was made to the curves of Hadley et al at the  $160^\circ$  point and the fit was found to be excellent over most of the angular range. Between  $172^\circ$  and  $176^\circ$ , however, the 90 Mev data appears to flatten off, in good agreement with Strauch (abstract, Cambridge A.P.S. meetings), and in qualitative agreement with R. Fox (thesis). The 310 Mev data shows no such flattening as far in as  $176^\circ$ . An experiment has been planned to measure the  $180^\circ$  scattering at both energies to check these points.

### 19. Low Energy Meson Nucleon Interaction

O. Heinz

The experiment on the low energy meson-nucleon interaction has been concluded and analysis of the data is now in progress. There is no evidence of an increase in the meson production cross section in the reaction  $p + p \rightarrow \pi^+ + p + n$  in the neighborhood of 22 Mev. This measurement cannot distinguish a small decrease in the production cross section since the absolute magnitude of the cross section is already very small.

### 20. Multiple Small Angle Scattering Measurements

S. Whetstone

New microscope stages have been secured in preparation for multiple scattering measurements in nuclear emulsions. Measurements to estimate stage "noise" have been undertaken.

---

2. W. E. Crandall, UCRL-1637.

## 21. Attenuation of Positive Pion in H<sub>2</sub>

S. Leonard and D. Stork

During the last three months instrumentation on this experiment has been completed. We have had an one two-day cyclotron run and are now analyzing the data gathered at that time in the form of photographs of the oscilloscope screen on continuously moving 35 millimeter film. The experimental setup and method has been described earlier. The data on the as yet unread film will make possible the determination of the attenuation cross section in liquid hydrogen for positive pions of about 33, 44, 56 and 71.5 Mev.

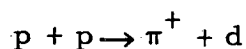
## 22. Pion Production by Protons on Carbon at 180° to the Beam

S. Leonard

During the past three months the work on this experiment has been virtually completed. An additional measurement of the production cross section for positive and negative 9 Mev pions has been made, using the nuclear emulsion detection method described earlier. This last measurement is not quite finished. The results, corrected for errors due to the thickness of the production target, decay in flight and nuclear absorption in the absorber plate holder, are:

<u>For <math>\pi^+</math></u>		<u>For <math>\pi^-</math></u>	
$\pi$	$d\sigma/d\Omega dE \text{ cm}^2/\text{Mev, ster, nucleus}$	$\pi$	$d\sigma/d\Omega dE \frac{\text{cm}^2}{\text{Mev, ster, nucleus}}$
18 ± 1.6	$3.61 \pm 0.35 \times 10^{-30}$	18 ± 2.3	$2.47 \pm 0.47 \times 10^{-31}$
32 ± 1.7	$3.13 \pm 0.25$	32 ± 2.0	$2.31 \pm 0.32$
51.5 ± 1.2	$1.64 \pm 0.16$	51.5 ± 2.0	$1.50 \pm 0.29$
74 ± 5.3	$0.76 \pm 0.08$	74 ± 4.3	$0.30 \pm 0.12$
118 ± 8.0	$0.09 \pm 0.03$		

An attempt is being made to relate the measured cross sections for proton on carbon to the cross section for the reaction:



as measured for free nucleons by Cartwright, Whitehead, Richman and Wilcox.

## 23. Total Positive Pion Cross Sections in Complex Nuclei

D. Stork

The data from a December cyclotron run have been analyzed and the following results for the measured attenuation cross section divided by nuclear area have been obtained:

Attenuation Target	Mean Pion Energy in Target		
	33 Mev	46 Mev	67 Mev
Beryllium	0.32 ± 0.04	0.57 ± 0.04	0.69 ± 0.04
Carbon	0.31 ± 0.05	0.63 ± 0.04	0.67 ± 0.05
Aluminum	--	0.71 ± 0.05	0.88 ± 0.06
Copper	--	0.65 ± 0.07	0.82 ± 0.06

The half angle of acceptance of the 14 inch back counter was  $35^\circ$ . Thus the measured cross section is  $(1 - F) \sigma_a + \sigma_s$  ( $\theta > 35^\circ$ ), where  $\sigma_a$  is the interaction cross section,  $\sigma_s$  is the elastic scattering cross section and F is the efficiency of the back counter for counting ionizing prongs from an interaction event. The leveling off and dropping of the measured cross section divided by nuclear area is due to the forward peaking of the diffraction scattering for the heavier nuclei. A complex square well model is being studied by means of partial wave analysis in order to separate  $\sigma_a$  and  $\sigma_s$  from the measured cross sections. A preliminary estimate of the pion mean free path for interaction in nuclear matter shows a strong energy dependence, approximately as  $(p_\pi)^4$ . This seems to reflect directly the excitation function for the free nucleon-pion interaction. Further data were obtained in February and are now being analyzed.

#### 24. Excitation Function for $p + C_{12} \rightarrow \pi^+$

D. Hamlin and J. Merritt

Work is in progress on the excitation function for the reaction  $p + C_{12} \rightarrow \pi^+$ . A preliminary cyclotron run indicated that detection of the mesons at  $90^\circ$  or  $135^\circ$  is not feasible without the use of a magnet. On a subsequent run magnetic separation was used to observe the mesons emitted at  $90^\circ$  for several proton beam energies. Results are being analyzed and more runs are planned.

#### 25. Measurements of the Absolute Meson Production Cross Sections

W. Dudziak and R. Sagane

The experiment on  $\pi^+$  and  $\pi^-$  meson production cross sections resulting from the interaction of 340 Mev protons with carbon indicates that at zero degrees to the proton beam the  $\pi^+/\pi^-$  ratio will never be smaller than 12. This, of course, neglects consideration of the Coulomb effect at very low meson energies. The ratio is 12 at a  $T_\pi = 15$  Mev and continues to increase to infinity with meson energy. As a result the once proposed variation of this  $\pi^+/\pi^-$  (i. e., variation as  $A + Z/A - Z$ ) is far from being correct even if corrected for the Pauli exclusion principle as indicated by Chew and Steinberger. This large ratio as well as the recent experiments of Powell, Ford and Neher seem to indicate that meson production processes in complex nuclei are more favorable when a deuteron is formed during the production process as is the case in free proton-proton collisions. This idea was once proposed independently by Richman and Dudziak when preliminary experiments indicated the existence of such large ratios.

The calibration spectrum for the 22-inch spiral orbit spectrometer is near complete. This is a spectra of  $\pi^+$  meson production cross sections versus meson energy from carbon at  $90^\circ$  to the proton beam. This information on  $\pi^+$  meson production has already been published by Richman-Wilcox and also by the Columbia group (Passman, Block, Havens). The published Berkeley and Columbia data are in disagreement. It has, however, been found that part of this disagreement is caused by the different  $(dE/dx)$  which is used in the calculation of the cross section by the different groups. This discrepancy increases with meson energy so that at a meson energy of  $T_\pi = 130$  Mev it is as large as 67 percent and is therefore one factor which contributes to a higher cross section as reported by the Columbia group. The new results have been carried out to a much greater accuracy than that reported by either group. The new data falls in between the Richman-Wilcox and Columbia data at low meson energies and is in agreement with the Richman-Wilcox data at energies above  $T_\pi = 70$  Mev.

Preliminary experiments on measurement of  $\pi^+$  and  $\pi^-$  meson production cross sections have been made using the 22-inch spiral orbit spectrometer. This included the study of the shape of the magnetic field distribution at the stable orbit, effect of the position of the main energy degrader, effect of radial and vertical focusing and the effect of final degrader. As a result of these experiments, many new problems have arisen which will require a much greater effort in the development of the instrument before it can be used most efficiently. However, sufficient information has been obtained so that one can at present conduct experiments using the spiral orbit principle. As a result the  $\pi^+$  and  $\pi^-$  function of  $Z$  resulting from proton bombardment along with the  $pd \rightarrow \pi^+/\pi^-$  experiment will be carried out before further development of the instrument is undertaken. Furthermore, measurements of production cross sections versus meson energy resulting from the interaction of the synchrotron gamma ray beam with protons and deuterons is now in progress. The low meson energy region (below  $T_\pi = 35$  Mev) is at present our chief interest.

## 26. Charged Particles from Heavy Elements

R. Eisberg and G. Igo.

In this quarter considerable progress has been made in the experimental program concerned with inelastic proton scattering from heavy elements. The final troubles have been removed from the remote control scattering chamber and its associated pumping system. This device is now being put into general use as a linear accelerator research tool, since several other experiments in addition to ours have been designed to make use of its facilities. At the beginning of the quarter some data was taken on the inelastic spectrum from Pb at  $90^\circ$ . The results were reported at the Pasadena meeting of the American Physical Society. About this time, however, we came across the theory of Landau concerning the statistical fluctuation in the ionization of charged particles. His calculation explained the surprisingly wide distribution in pulse heights from our proportional counter when traversed by monoenergetic protons and, in fact, our proportional counter data provided the first experimental verification of Landau's theory in the heavily ionizing region. These results were published in UCRL-2031 and are to appear in the Physical Review.

The very wide statistical distribution appeared at first to frustrate our attempt to identify the mass of the scattered particles, we were detecting, by correlating  $dE/dx$  and  $E$ . However, it was proposed that we use several proportional counters to sample the ionization and then take the smallest pulse. A system has been constructed consisting of three proportional counters and a simple circuit to select the smallest pulse. This has been partially tested and appears to work quite well. Soon we expect to be back taking more data on the inelastic proton spectra.

## 27. $p + p \rightarrow d + \pi^+$ Differential Cross Section

F. Crawford and M. Lynn Stevenson

The above reaction is being investigated with proton energies of 340, 335 and 327 Mev. The cross section is measured by detecting the meson and deuteron in coincidence. The angular distribution in the center of mass system at 335 Mev is:

$$\frac{d\sigma}{d\Omega}(\theta) = 33 \left[ 0.32 (1 \pm 0.12) + \cos^2 \theta \right] \times 10^{-30} \text{ cm}^2 \text{ ster}^{-1}$$

The total cross section is:

$$\sigma_T = 2.7 (1 \pm 0.1) \times 10^{-28} \text{ cm}^2$$

The cross section for 327 Mev at  $90^\circ$  in the center of mass system is:

$$\frac{d\sigma}{d\Omega} = 7.6 (1 \pm 0.14) \times 10^{-30} \text{ cm}^2 / \text{ster.}$$

If one uses Schulz's excitation function at zero degrees and the value of the above cross section at 335 Mev at zero degrees to determine the cross section at 327 Mev at zero degrees, one finds that the angular distribution in the center of mass system at 327 Mev is:

$$\frac{d\sigma}{d\Omega}(\theta) = 26 \left[ 0.30 (1 \pm 0.20) + \cos^2 \theta \right] \times 10^{-30} \text{ cm}^2 \text{ ster.}$$

The total cross section is:

$$\sigma_T = 2.0 (1 \pm 0.15) \times 10^{-28} \text{ cm}^2$$

The above data have not as yet been corrected for  $\pi$ - $\mu$  decay in flight and other small systematic errors. Other data are now being analyzed at  $90^\circ$  in the center of mass system at 340 Mev and 327 Mev.

## 28. Beta Ray Spectrometer

R. Wallace

Drawings for the linear accelerator beta ray spectrometer have been nearly completed. The gray wedge pulse height analyzer has been completed



to a point where it can be used. A spectrum has been produced with it and compared to that produced electronically. The Exakta camera, loaned to us by Prof. Tobias, has been returned. With the Exakta it was possible to see single pulses, while with the camera still available to us it is possible to see only groups of ten or more pulses. A new wedge has been obtained, which appears to be of good quality.

### 29. Time of Flight Neutron Spectroscopy

W. Linlor and B. Ragent

Time of flight neutron attenuation experiments at flight distances of 145 feet and 489 feet using the neutrons from 180 Mev deuterons stripped on 4 inch beryllium have been carried out. Energy resolution at 90 Mev at these distances are (in terms of equivalent probable error) respectively 2.6 Mev and 0.8 Mev, due to width of probe pulse.

Results for lead are consistent with the "Harwell-dip" but the counting statistics uncertainty does not permit drawing of conclusions.

A run was made on December 20 and 21, 1952, at a distance of 68 meters, using only lead as the scatterer. The intention was to obtain sufficient data so as to resolve any small variations in total cross section with energy. Forty 100-foot reels of film were taken, which are currently being analyzed.

### 30. Synchrotron Studies

A. C. Helmholz

During this period, R. Madey, K. Bandtel and W. Frank have had a number of runs investigating the photomesons from deuterium. Their latest runs have studied the energy distribution of the protons in coincidence with  $\pi^-$  mesons with the idea of determining the magnitude of the spin-flip cross section. In order to interpret the data, a good deal of theoretical work is necessary and this is being done at the present time. When this is complete, the experimental data can then be interpreted in terms of a spin-flip cross section.

Barkas and several others have exposed plates to the synchrotron beam to look for some of the star producing particles which have been found at Cal Tech. None were found in agreement with the results at Cal Tech, which indicates that the cross section for their production becomes appreciable only well above 350 Mev.

S. White and N. Jarmie made a long run exposing plates to the  $\pi^+$  mesons at zero degrees to the  $\gamma$ -ray beam. Their targets were both hydrogen and deuterium. Some of the plates from the hydrogen runs were suitable for scanning and the preliminary results indicate that the cross section for photoproduction at zero degrees is very small. The detailed results will probably be available in the next month. The plates from deuterium are also being looked at.

R. Post and C. McDonald have looked at the time distribution of particles in  $\gamma$ -produced showers. However, their results are very incomplete.

N. Lewis and F. Coensgen have made two runs looking for elastically scattered  $\gamma$ -rays from a number of elements. Since the cross section is very low for this process (they are looking in the region of 15-30 Mev), no definite indications of positive results have come out. However, a more sensitive set up will be tried in the near future.

A good deal of work on the calibration of the machine has been done, indicating fair agreement with the results of the test with the Cornell chamber. The old calibration of Blocker and Kenney is probably too high, that is, gives too many Q per Nunan for the present set up of the Nunan chamber. A new measuring chamber will probably have to be devised because of the influence of background radiation.

### 31. Theoretical Group

David L. Judd

#### Differential Cross Section for $p + d \rightarrow \pi^+ + t$ . S. Bludman

A calculation of the differential cross section has been made for the reaction  $p + d \rightarrow \pi^+ + t$ , using more accurate deuteron and triton wave functions than those employed in the calculation published by Ruderman some time ago. Very satisfactory agreement with experiments recently performed at this laboratory was obtained by introducing a "hard core" to suppress high momentum components of the deuteron wave function.

#### Treatment of Meson-Nucleon Scattering and Photo-Production. S. Gasiorowicz

A general phenomenological calculation of meson-nucleon scattering and photo-production is in progress, treating S states and all P states, except the one of isotopic spin and total angular momentum  $3/2$ , by weak coupling theory applied to a Hamiltonian containing a pair term treated exactly and a pseudovector term treated by perturbation theory. The  $I = J = 3/2$  state is being treated by the Wigner-Eisenbud formalism applied to a Klein-Gordon equation. Numerical results are not yet available for scattering; however, a good fit of the charged photomeson production angular distribution has been obtained by the inclusion of a quadropole term which have been omitted in treatments by other workers.

#### $\pi^-$ Production Cross Section. B. Macdonald

A calculation of  $\pi^-$  meson production in n-d collisions has been initiated during the period covered by this report but is not yet concluded. The calculation is being made by integrating the measured excitation function of the reaction  $p + p \rightarrow \pi^+ + d$  over a deuteron momentum distribution, and assuming charge symmetry.

#### Pion Production from Complex Nuclei. S. Bludman

The production of  $\pi^+$  mesons by protons on complex nuclei, as mentioned in the preceding quarterly report, is being calculated for several

incident proton energies and meson angles in the laboratory system, using the  $p + p \rightarrow \pi^+ + d$  excitation function and angular distribution. Numerical results for the energy spectrum of mesons at  $90^\circ$  due to 340 Mev protons will soon be available.

#### Studies of Nucleon Electromagnetic Field. L. Smith

Calculations have been made of the decay of the neutral  $\pi$ -meson into a  $\gamma$ -ray and a pair, and into two pairs, using the neutral meson-electromagnetic field interaction terms which Schwinger devised by an approximate elimination of the proton field. Some consideration was given to higher order nucleon effects, particularly the influence of an anomalous magnetic moment and processes of higher order in the meson-nucleon coupling constant. It was concluded that such details only alter the effective meson-electromagnetic field coupling constant, and thereby the absolute value of the lifetime, but not the relative probabilities of the three modes of decay, or the energy and angular distributions of the decay particles.

The decay into two pairs offers, in principle, a means of determining the parity of the neutral meson because the planes of the two pairs are correlated in the same manner as the polarization vectors in the predominant two photon decay. However, the process is so rare (about 1 in  $10^4$ ) and the correlation so slight that the measurement would be still more difficult than a determination of the polarization of the two photons by double scattering.

#### Negative Pions in Hydrogen. S. Tamor

A study of the internal conversion of negative pions in hydrogen has indicated that about 1 percent of the gamma rays convert into pairs, independently of the form of meson theory employed. However, a detailed experimental investigation is regarded as unprofitable.

Calculations of radiative corrections to meson-nucleon scattering in the radiation damping theory are continuing.

#### Nucleon Scattering. R. Huddleston, F. J. Vaughn and W. Heckrotte

Compton scattering on nucleons is being investigated using the classical model of an extended nucleon source coupled to a pseudoscalar field. Work is continuing on the high energy deuteron photodisintegration by pseudoscalar weak coupling theory. The energy distribution of the charge-exchange neutron beam produced in a target by the cyclotron beam of protons is being studied. The total neutron cross section as a function of element and energy is being investigated. A tentative calculation, using an energy-dependent potential well, yields a fair agreement for lead in the energy region from 20 to 140 Mev.

#### Polarization Effect on Nucleons. J. V. Lepore and W. Heckrotte

Nucleons elastically scattered from nuclei should be partially polarized by the strong spin-orbit force underlying the shell model predictions. Should the polarization be large at small angles a relatively good source of polarized particles would be available. The effect would depend strongly on the choice of target nucleus. An attempt to survey the possibility of calculating this effect was made, with the hope that the interior region of the nucleus

could be represented by a spin-dependent complex index of refraction. However, it appeared necessary to carry out a phase shift analysis which would be laborious for moderate energies and nuclear sizes, and no detailed calculations have yet been undertaken. The amount of polarization should depend rather sensitively on the model chosen for the spin-orbit potential and on its parameters.

#### Charged Scalar Meson Field. B. D. Fried and R. J. Riddell

The Tomonaga intermediate coupling approximation is being studied for charged scalar, neutral pseudoscalar, and charged pseudoscalar meson theories. Numerical calculations of the eigenvalues and eigenvectors of the Tomonaga hamiltonian have been carried out in these three cases for the ground state and several excited states. Higher order corrections to the Tomonaga approximation are being computed in order to estimate the validity of the formalism. The application of this method to meson scattering is under investigation.

A combinatorial enumeration of the number of Feynman diagrams corresponding to processes of any order of a perturbation expansion has been carried out. The asymptotic forms of the expressions obtained make it seem doubtful that the expansions can converge.

#### Treatment of Symmetrical Pseudoscalar Field. J. V. Lepore

The past quarter has been spent in studying, in collaboration with other members of the theoretical group, the consequences, for meson-nucleon processes, of the symmetrical pseudoscalar theory in the approximation of treating the nucleon as an extended source. A simple proof has been given of the fact well known from the strong coupling theory that the first excited state of the single nucleon system (bound or virtual) is associated with spin and isotopic spin  $3/2$ . This same model shows that a resonance formalism based on a Klein-Gordon equation leads to Breit-Wigner type formulae which vary more rapidly with energy than those predicted in the usual theory. This has as a consequence that cross sections for processes, such as meson-nucleon scattering, photo meson production will fall off more rapidly with energy above resonance than would be expected on the basis of the non-relativistic Breit-Wigner formalism employed by Watson and Brueckner in their studies of these processes. This seems to be in agreement with the general trend of the data on neutral photo meson production obtained at California Institute of Technology.

Work is under way in collaboration with Neuman on the calculation of the scattering of low energy electrons by a Coulomb field.

#### Nucleon-Meson Interaction Theory. R. Arnowitt

Using the techniques of Schwinger, the Green's function equation governing the interaction of a nucleon with a meson has been set up. The wave function for the nucleon-meson system obeys the corresponding homogeneous equation. If one makes an adiabatic approximation on the interaction operator that appears in the equation, the two time wave function can be reduced to an ordinary single time function which obeys an equation with a sum Hamiltonian. The lowest order interactions correspond to the two "Compton scattering" graphs. The graph which has only a nucleon present in the intermediate state

(and hence yields interactions only in the isotopic spin  $1/2$  state) gives a repulsive delta function potential. The other graph (where crossed mesons appear), upon a non-relativistic reduction, gives a central and spin-orbit potential of range  $\sim 1/3\mu$ . In particular, interest centers around the possibility of the existence of bound states which might be viewed as isobars. Approximate solutions of the equation are being considered to study this possibility.

#### Synchrotron Phase Stability. L. Smith

The loss of phase stability in very high energy proton synchrotrons using alternating gradient focusing has been studied using the UCRL differential analyzer. It was concluded that counteracting the undesirable properties of this effect would not be difficult in practice.

#### Study of Beam Extraction in Synchrocyclotron. H. H. Hall

Work on beam extraction in synchrocyclotrons has continued. Alternatives to the regenerative peeler-deflector system are under examination. A proposal to produce transient local magnetic field variations by means of very large pulsed currents is under consideration, and catching efficiencies have been estimated. A study was made of a proposal to extract the beam by neutralizing it with electrons. It was found that extremely high electron plasma densities would be required. Estimates of desirable foil thicknesses for use in a scattering deflector have been made.

#### Bevatron Inflector. L. Smith

The problem of determining the shape of the bevatron inflector electrode to provide a sufficiently uniform field in the channel has been completed. In the narrow tip of the inflector it is necessary to add certain ridges to the high voltage electrode above and below the beam, while in the main body of the inflector a flat electrode should be sufficient. Also the tolerance on the deviation of the faces of the bevatron accelerating electrode from parallelism, found in UCRL-547 to be quite stringent, has been reconsidered by a different method which again leads to the same result.

#### Study of Alternating Gradient Focusing. D. L. Judd

A number of calculations relative to alternating gradient focusing are in progress. A parametric study of lens systems of this type for handling accelerator output beams is under way. Certain resonant and non-linear effects arising in this type of system are being investigated, particularly those of the fairly large non-linearities in the phase-reversal focusing proposal of M. Good for linear accelerators. It appears that such effects need not lead to loss of stability.

Theoretical estimates have been made of some problems of free molecular streaming and of geometrical effects in connection with the Laboratory's ion pump development program.

## II. ACCELERATOR OPERATION AND DEVELOPMENT

### 1. 184-inch Cyclotron Operation

J. Vale

The cyclotron was in operation very consistently during this period, averaging about 97 percent of the time that the crew was on duty. This implies, naturally, that there was a minimum of outage of all sorts.

Meanwhile, engineering is progressing on the conversion of the machine for increased energy. This phase of the program will be treated in the next quarterly report.

### 2. 60-inch Cyclotron Operation and Development

Operations. William B. Jones

The operation of the 60-inch cyclotron during this quarterly period was as follows:

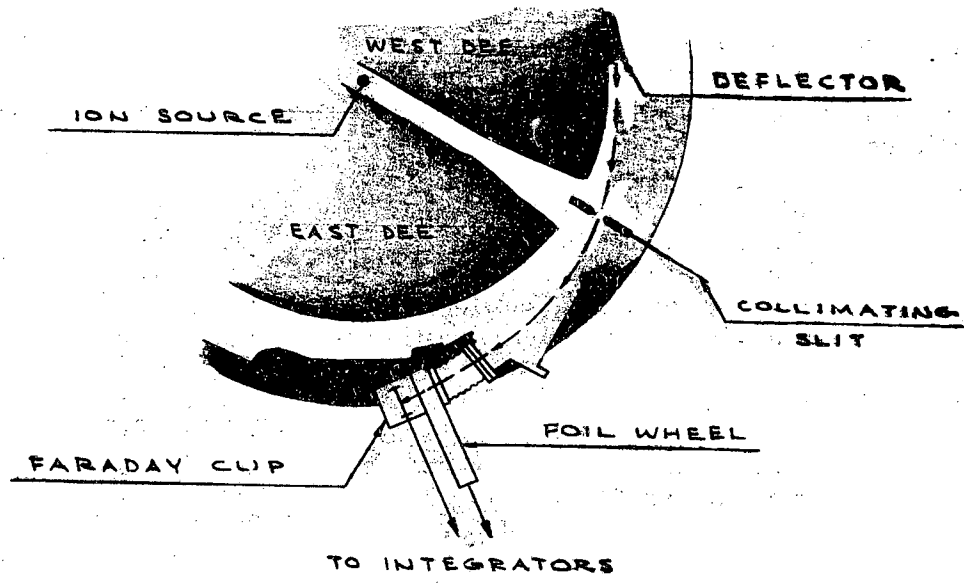
Alpha bombardments	302.0 hrs
Deuteron bombardments	84.0 hrs
Proton bombardments	308.0 hrs
Carbon bombardments	93.0 hrs
Development and experiments	102.5 hrs
TOTAL	<u>889.5 hrs</u>
Outage	210.5 hrs
TOTAL	<u>1100.0 hrs</u>
Shutdown	988.0 hrs
Holiday shutdown	120.0 hrs
	<u>2208.0 hrs</u>

Operating efficiency: 80.9 percent

Some users of the 60-inch cyclotron beams have questioned the energy stability over protracted periods of time, resulting from parametric adjustments. Range measurements of the beam versus dee voltage taken some time ago indicated a variation of 39.6 Mev to 40.2 Mev at the low and high voltage extremes applied to the dees.

With the physical setup illustrated in Fig. 1, the beam range in aluminum was taken for various positions of the collimating slot and north and south motion of the ion source. The results are as follows:

- 1) With the ion source 1/2 inch north of geometric center, the range was 161.7 mg/cm<sup>2</sup> (39.2 Mev). No measurable variation occurred in 7/16 inch horizontal scanning of the beam.



MU-5040

Fig. 1

- 2) With the ion source 1 1/2 inches north of geometric center, the range was 168 mg/cm<sup>2</sup> (40.1 Mev) with no measurable variance over the 7/16 inch scanning.

These initial measurements indicate a high order of energy selectivity of the deflecting system under constant parameters but two to three percent variation in energy results from parameter changes. As time permits, further studies are anticipated.

The cross-dee or grid feelers (UCRL-2054) were removed and replaced with the flat type (UCRL-1729, p. 39). The change was made to re-establish the carbon beam intensities experienced with the flat type. Carbon beams have been attained of 30 to 40 x 10<sup>-9</sup> amperes (internally). Nonetheless, the sharp beam increases of other ions reported have been lost with return to the flat feelers. A feeler design is being considered to compromise the needs of the carbon ions and other particles.

#### Internal Beam Monitoring. G. Bernard Rossi

At present cyclotrons of the c.w. type that have large circulating beams (0.5 to 1.0 milliamperes) experience considerable difficulties in monitoring these beams electronically. These difficulties include the presence of large amounts of rf pickup from the dees, the need for adequate insulation of target-cooling water and target destruction potentialities. The electronic monitor has eliminated the thermal lag times that occur with present thermopile measuring methods. This lag is always troublesome when beam maximizing is being attempted, since evaluation is delayed. At times the effects of adjustments are completely masked. In practice, it is necessary to use the external electronic monitoring system to peak the beam before switching to internal targets and thermopile device.

The internal target experiments (outlined in UCRL-2054), where severe beam limitations are encountered, require a fast monitoring method. To provide this speed, it is necessary to have an insulated target holder which is shielded from the dee rf fields. Shielding becomes a problem from two points of view:

- 1) Beam intensities of 1 ma at 20 Mev represent 20 kw of power to be dissipated by the shield and target, requiring adequate cooling for both.
- 2) The shield must be thick enough to limit energy degradation to a small quantity, i. e.,  $> 1$  Mev.

To avoid these difficulties, a shield was prepared of 3 1/2 inch o.d. copper tubing. See Figure 2. The target region was cut back along the beam median line, providing a slot slightly less than the beam height and long enough to allow the target to be positioned away from rf field penetrating regions. If the spacings  $l$  and  $D$  are larger than  $h$ , the field penetration should be less than  $1/e$  of the surface value and rf pickup should be minimized.

Measurements made with this shielded probe indicated that a 10 percent error exists between the thermal and electronic current values, the electronic measurement being higher. This difference appeared as a base



reading on the probe, the first presumption being that it represented rf pick-up. Further investigation indicated it was due to ions accelerated by the dees after being stripped by P. I. G. electrons oscillating between the dees. Evidence for this assertion appeared when this pickup varied directly with gas pressure (tracking closely with the pressure ion gauge) and varied with magnetic field (peaking at various field values). It was found that these particles were of low energy by attempting to measure them with the thermal system, which is sensitive to energy and not charge. No variations were evident in the thermal-monitored current despite field changes or large variations of tank pressure. A shielded water-cooled probe assembly has been designed around these parameters for general use with internal beams. Some of the design features are discussed subsequently by C. A. Corum.

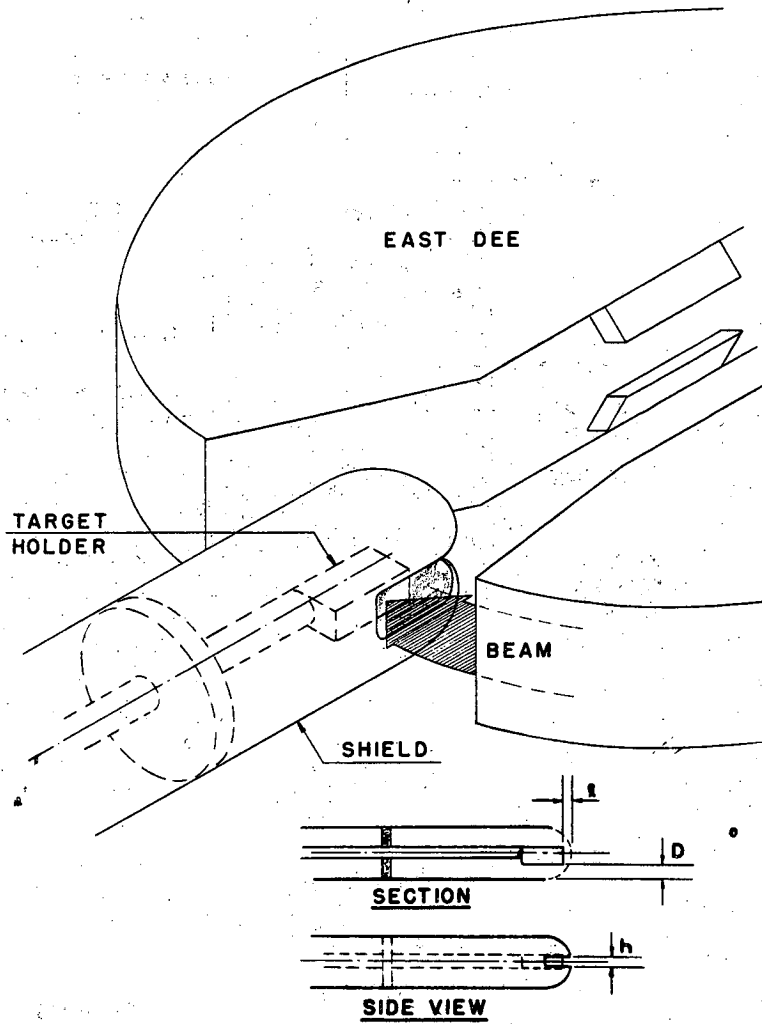
#### RF Shielded Minature Foil Target. Charles A. Corum

A new unit has been designed, based upon the results of the rf shield experiment and a later development of the cylindrical target of the internal beam probe (UCRL-2054). This unit presents a target holder and an rf shield (both water-cooled) for bombarding foils in the internal beam, thus allowing electronic measurement of currents. (See Figures 3, 4, 5 and 6). The target holder is triangular in shape and holds the foil target at right angles to the beam, presenting a constant target thickness over the width of the beam. A screw in back of the target holder actuates a wing-type nut which automatically grabs and applies pressure to a strap band. The band forces the target foil back against the gaskets making a water and vacuum seal. Lucite spacers insulate the target holder and target water lines from the supporting tube on which the rf shield is mounted. The rf shield water connection is made by the water tubing ends passing through two "O" rings retained in the shield plate. Standard rf finger stripping, mounted on the shield plate, contacts and grounds the shield.

For quick disassembly, which is necessary for personnel radiation protection, the shield can be pulled off after loosening two screws, exposing the target holder. Turning the screw (located in back of the target holder) disengages the nut holding the strap band, allowing both the band and the target to be removed. Special long-handled screwdrivers are available so that the unit can be disassembled from a distance of approximately three feet. If the target is too hot for immediate handling and it is necessary to remove the target holder block with the foil and strap intact, only two screws need to be loosened to free the block for removal.

#### Flat Dees. Charles A. Corum

A new set of dees have been fabricated for use in the 60-inch cyclotron. See Figure 7. Started in March, 1952, the design has resulted in a simpler unit than the existing set. One-piece construction, requiring large bulky spinings, has been replaced by flat sections; soldering between upper and lower section has been replaced with mechanical joining; perforated joining plates, allowing better pumpout, has replaced solid construction; outside stem to dee clamps have been supplanted with internal clamping to allow greater pumping clearance through the narrow stem throat region; a dee height reduction of  $3/4$  inch will allow installation of internal Rose shims when desired. A dee weight reduction of about one-third is anticipated from metal choices. The bronze clamp members were replaced with 24 ST aluminum. The support



MU-5042

Fig. 2

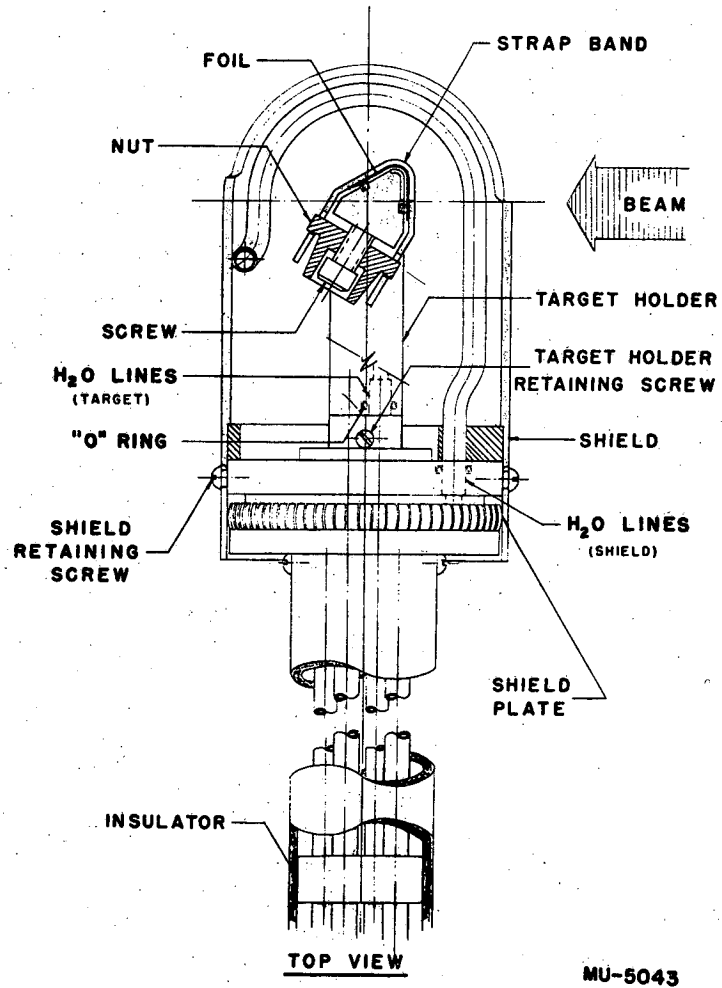


Fig. 3

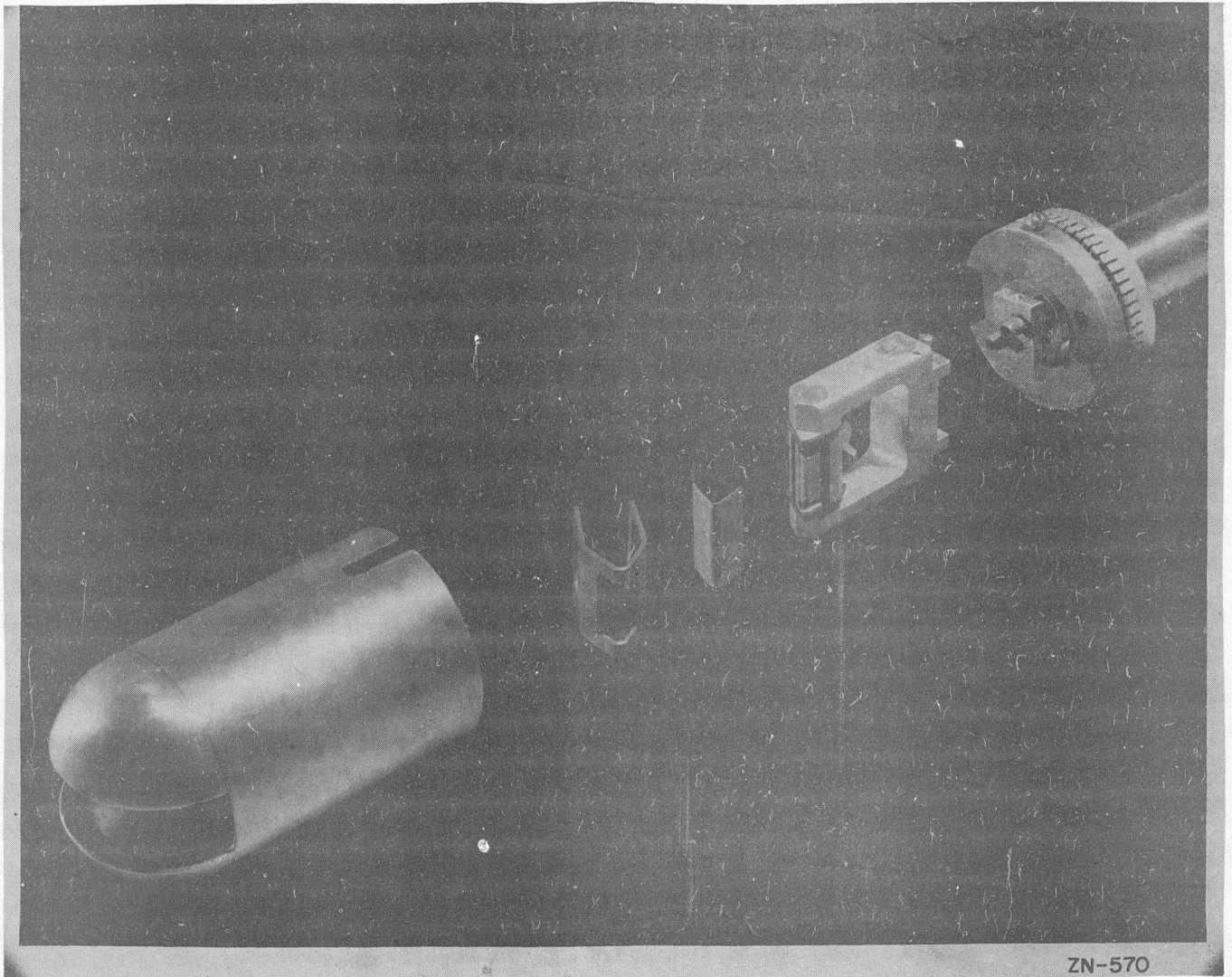
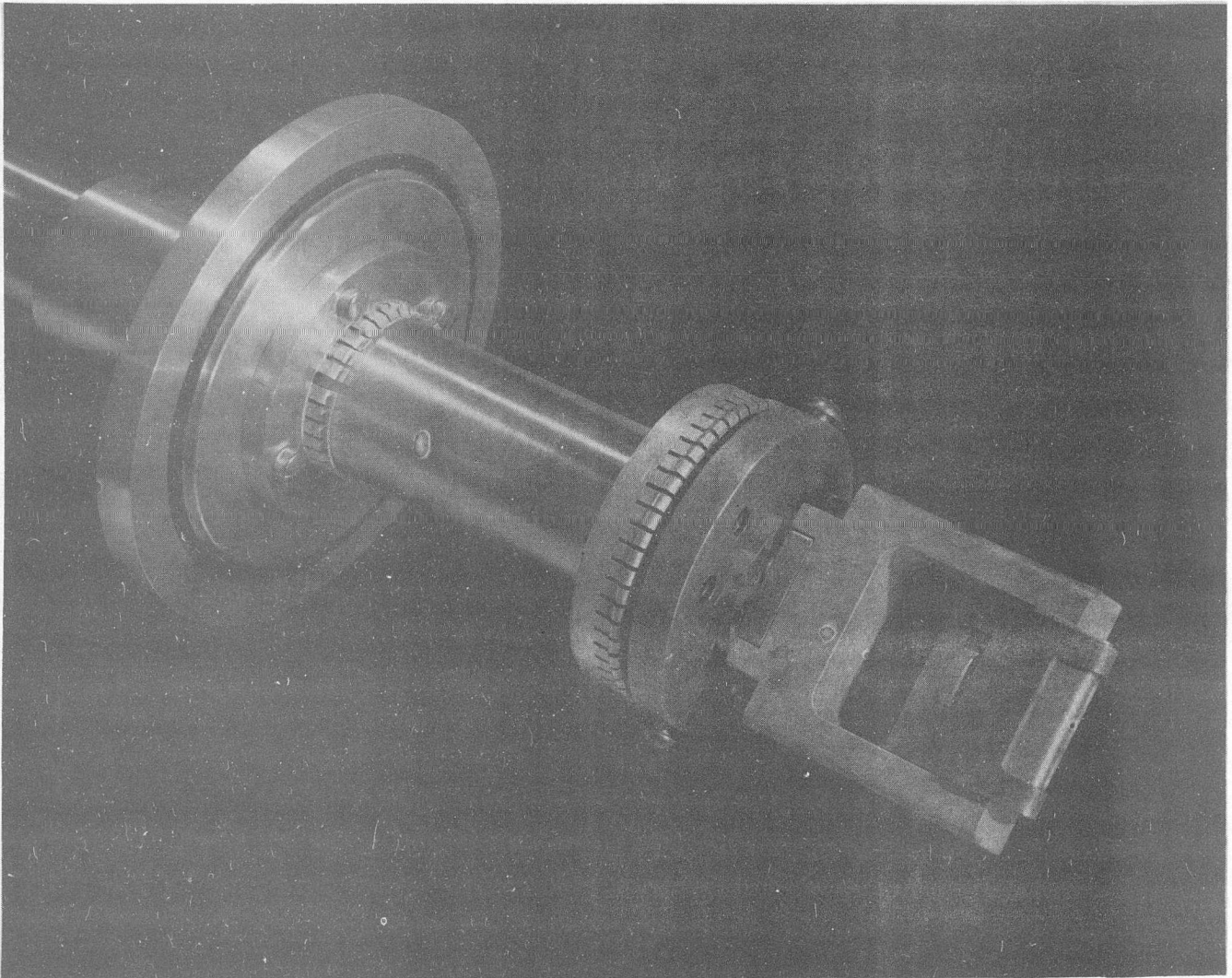


Fig. 4



ZN-569

Fig. 5



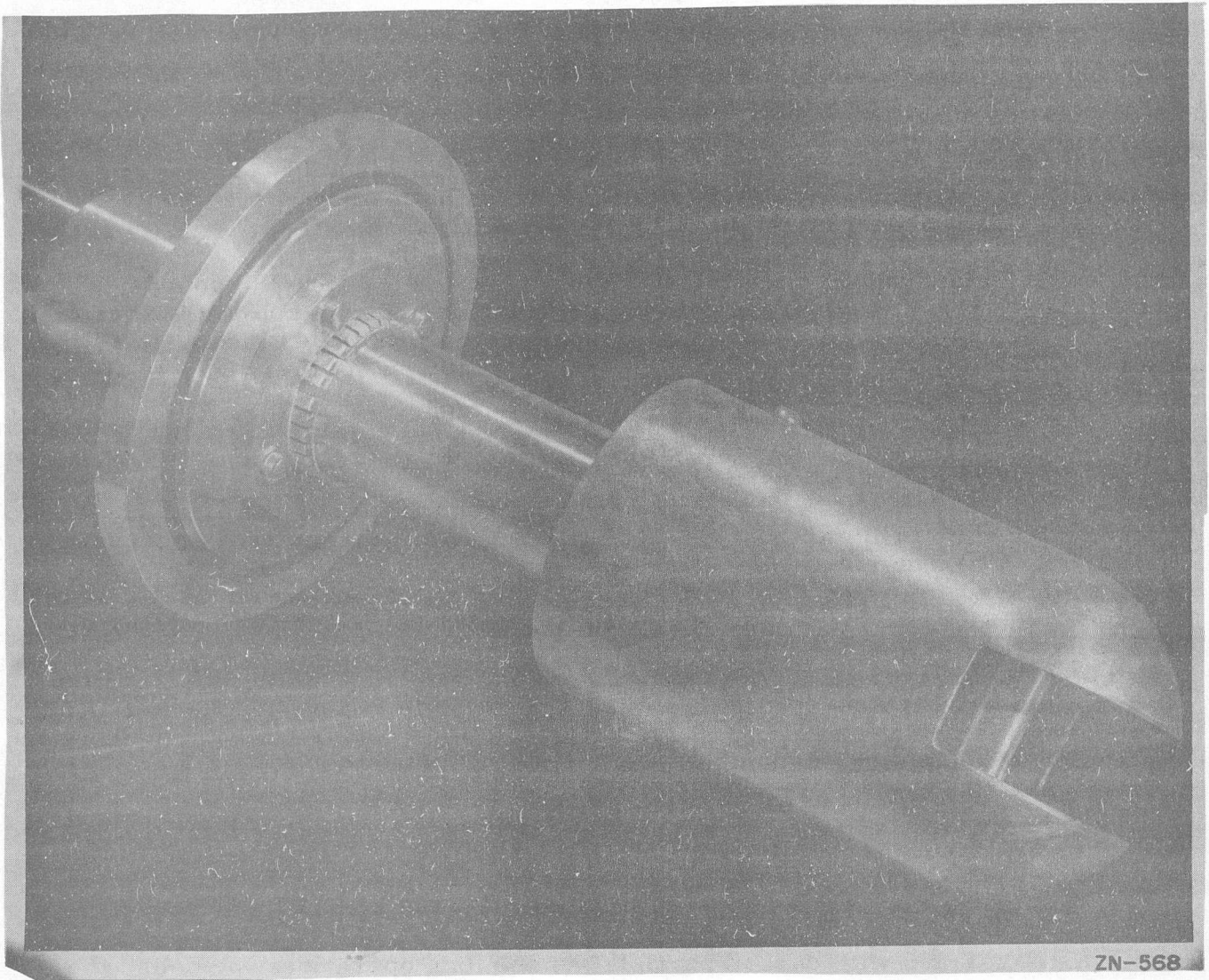


Fig. 6

area, however, has been increased by about a factor of three. The new dee height is 4 inches along the entire length. This allows mirror image dee surfaces to be mechanically joined by perforated separation plates. The 26 1/2 inch maximum radius was maintained as well as the 25 inch exit radius and 30 inch curvature.

The basic rf clamp design was preserved as reported in UCRL-627, p. 36 and illustrated therein in Figure 1. This clamp is six inches in diameter and contains 30 water-cooled fingers. The transition from this clamp to the dee was formed from 1/8 inch copper sheet copper-welded to the dee plate.

The ion acceptance dee has removable feelers but their adjustable aspects have been eliminated; the deflector dee has been designed to allow installation of feelers also, if desired. The adjustable dee wall facing the deflector was also eliminated since after three years of use it has proven to be of dubious value. The present status of these dees is that they must be "drydocked" before installation. Plans call for the assembly of dees and stems external to the machine so that the entire assembly can be checked with 100 lbs. of helium before installation.

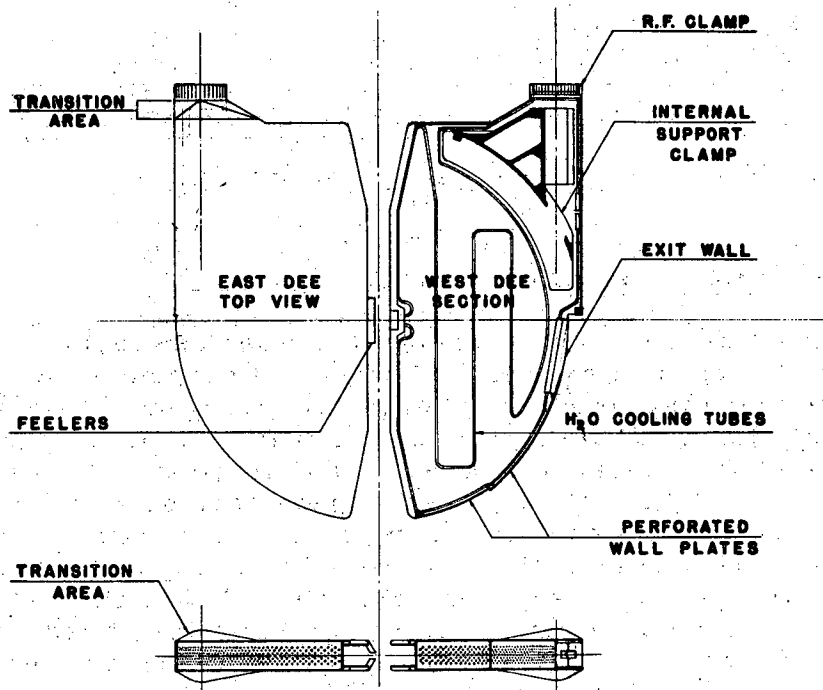
Soft copper sheeting, 1/8 inch thick and totaling 288 pounds, was used in the dee surface preparation. The surface and rim cooling was provided by 110 inches of 3/8 inch o.d. copper tubing with 0.049 inch wall. To bind the cooling lines to the dee inner surface, 100 oz. of Easy-Flo solder was used.

#### Carbon Ion Source. G. Bernard Rossi

Reference has been made in past reports to the use of graphite for ion source structures. It was used mostly with experimental sources, involved in carbon ion acceleration, to avoid using complicated water-cooling schemes. In cones used until recently, the so-called carbon "hat", which functioned as an electron catcher, becomes white-hot. Various metals, including tantalum and tungsten, were inserted into these hats to decrease the erosion life. In the cases of tantalum and tungsten, molten masses resulted which indicated that temperatures were generated in excess of 3300°C. With this temperature the hats had a life ranging between 6 and 10 hours, with replacement consuming one hour of change time plus varying amounts of operation "reset" time. The possibility also existed that the heated graphite was supplying the carbon atoms for the arc through sublimation of the hat material.

A copper cone was constructed to eliminate all carbon from the source to allay the erosion and sublimation. Figure 8 shows this source.

Tried with carbon particles under long operational periods, the cone proved to be as good as the experimental carbon models. The vertical water columns, separating cone and hat structures, were made of 1/4 inch i.d. copper tubing with 0.049 inch wall. After 50 hours of operation, the cone was removed and the wall thicknesses measured. Only 0.013 inch remained of the wall and a deep set appeared in the water-cooled hat. This wearing of the support members occurred on the experimental models, which were made of uncooled 0.080 inch tungsten wire, and appears to be a sputter effect not related too closely with temperature.



MU-5044

Fig. 7



Since increased life and more consistent running time resulted, the copper model is now used for  $C_{12}^{+6}$ . By varying the choice of metals used in the structure, it seems probable that a longer operating time may be achieved.

### 3. Synchrotron Operation

George C. McFarland

The synchrotron continued to operate at high intensity levels during this report period. The pair spectrometer magnet turn table was installed permitting orientation at any angle with the synchrotron beam.

The linear accelerator has been used by the physics research group while work is under way in preparation for using the linear accelerator as an injector for the synchrotron.

### 4. Linear Accelerator and Van de Graaff Operation

C. Nunan and R. Watt

#### Strong Focusing Conversion.

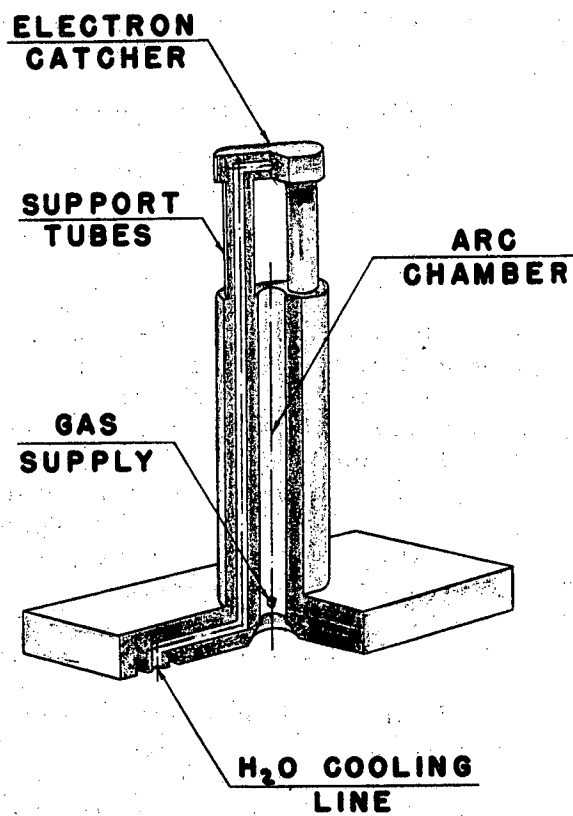
A system of four electrostatic lenses employing Brookhaven strong focusing was arranged convergent-divergent, divergent-convergent to a particle in the horizontal plane; and divergent-convergent, convergent-divergent in the vertical plane. The 4 Mev Van de Graaff proton beam was sent through the unexcited 40-foot linear accelerator, and filled to 3/4 inch aperture of the lens system. Mathematical analysis had previously indicated that with 44 kv between electrodes parallel particles in both vertical and horizontal planes should cross the axis at the same point at the end of the 20 inch long lens system. When the voltage was adjusted to 44 kv, the 3/4 inch Van de Graaff beam focused on a disc of quartz to a point less than 1/2 mm diameter. 85 percent of the beam was being accepted and focused as measured by a Faraday cup. Mathematical analysis shows that 100 percent of the beam in the horizontal components and 63 percent in the vertical components, or a total of 79 percent, should be accepted and focused. The 2 3/4 inch long electrodes are sections of hyperbolic cylinders milled to a few mils accuracy and spaced accurately to  $\pm 15$  mils. The axial spacing between electrodes equaled the electrode length. The copper electrodes are supported from copper cylinders by 3/4 inch long and 3/8 inch diameter steatite insulators and connected by RG-58/U cable.

#### Statistics.

Running time	53 percent
Installation of lenses and maintenance	31
Repair	16

#### Electrostatic Strong Focusing Installed in 32 Mev Proton Linear Accelerator.

Electrostatic strong focusing lenses with 2 cm aperture were installed in the 46 drift tubes of the linear accelerator and connected by poly-



MU-5041

Fig. 8

ethylene-insulated coaxial cables to three (+) and three (-) power supplies. Eight drift tubes were used per repeat length of the strong focusing force allowing an rf synchronous phase angle of about  $-9^\circ$  and requiring  $\pm 6$  to  $\pm 8$  kv to ground per electrode. The system was first tried on December 6, 1952, and an average beam current of  $0.5 \mu\text{a}$  was obtained with  $\pm 0.001$  radian maximum divergence. Previous values with grid focusing were  $0.25 \mu\text{a}$  and  $\pm 0.001$  radian. Lukewarm flow of cable insulation due to rf heating of the drift tube stems has caused several cable failures. The small synchronous phase angle has enforced small tolerances on cavity rf voltage and Van de Graaff injection voltage. It is planned to replace the polyethylene cable with teflon cable and operate with 6 drift tubes per repeat length of focusing force allowing a  $-16^\circ$  synchronous phase angle and requiring up to  $\pm 14$  kv per electrode.

## 5. Bevatron Development and Construction

W. M. Brobeck

### Magnet.

Final decision on the shape of the pole tip was reached during the period and the die has been completed and tested. A first shipment of the enameled pole tip plates was made from the supplier on January 30. Tests of the 1/7th scale magnet model indicated approximately two percent higher field obtainable than was the case with the 1/12th scale model. Tests have been run to determine the effect of the pole face windings in compensating for the shape of the residual field. These tests showed that good compensation could be obtained by connecting resistors across the windings so that the induced voltage in the windings would provide the necessary currents. Pole base slab assembly reached the 50 percent point at the end of the period. Installation of the first lower pole bases is to start early in February.

Westinghouse Company has decided to provide material and labor for connecting the magnet generators in series rather than in parallel and this change is now being made. A filter is planned to reduce the 12 and 24 phase ripple sufficiently to prevent interference with frequency tracking or appreciable increase in phase oscillation. The acoustical treatment for the generators has been completed. Operation of the generators to check the acoustical treatment and the effect of filtering is planned during February.

### Vacuum System.

Two tanks for the straight sections have been received, one of which has been installed and under vacuum since early in January. A pressure of two millimicrons was reached on an untrapped gauge in the empty tank. The tank has been loaded with parts to be installed in the quadrants and a pressure of four millimicrons reached with the pumping speed equivalent to the value that will be realized in operation. One curve tank has been completed and the top of two and the bottom of one other have been finished. Construction of the sides will be deferred until the first tank is installed which should be about the end of February.

Injector.

The Cockcroft-Walton high voltage supply for the ion gun had given considerable trouble, apparently from contamination of the oil used to insulate the high voltage parts. It was decided, therefore, to go ahead with an air insulated supply to avoid these difficulties as space was available for its installation. The frequency of the power supply is also being changed from 100 kilocycles to 800 cycles to reduce losses and simplify tuning. The first units of this supply were being tested at the end of the period. Completion of the ion gun and linear accelerator ready for test is being determined by the number of electricians available for the job. At present it appears that testing will start during the latter part of March.

Accelerating System.

The design work is nearing completion on the accelerating electrode. The saturable reactor system for tuning the electrode is being tested and housings for the final reactors are in the shop. It is hoped that tests in the straight section can begin during March.

Miscellaneous.

An increase in funds of \$337,000 has been received to provide for the estimated over run of about \$300,000 above the original \$9,000,000 appropriation. This figure does not include allowance for contingencies.

Plans are being made for shielding close to the magnet over about three-fourths of the circumference along the lines indicated by the results of the operation at Brookhaven. It is hoped that orders can be placed after the first of July. Shielding is not included with the scope of the present project.

A study is being made of a deflecting system for the protons which looks encouraging. The beam would be slowed down in an absorber placed at the outer radius and would spiral inward to a deflecting magnet where it would be bent outward again to leave the magnet through one of the straight sections.